Geomechanics and Engineering, *Vol. 28, No. 1 (2022) 49-64*
https://doi.org/10.12989/gae.2022.28.1.049

Effect of the variable visco-Pasternak foundations on the bending and dynamic behaviors of FG plates using integral HSDT model

Habib Hebali[1,2], Abdelbaki Chikh[1,3], Abdelmoumen Anis Bousahla[4], Fouad Bourada[1,5], Abdeldjebbar Tounsi*[1], Kouider Halim Benrahou[1], Muzamal Hussain[6] and Abdelouahed Tounsi[1,7,8,9]

[1]*Material and Hydrology Laboratory, University of Sidi Bel Abbes, Faculty of Tech nology, Civil Engineering Department, Algeria*
[2]*Departement of Civil Engineering, University Mustapha Stambouli of Mascara, Algeria*
[3]*Université Ibn Khaldoun, BP 78 Zaaroura, 14000 Tiaret, Algérie*
[4]*Laboratoire de Modélisation et Simulation Multi-échelle, Université de Sidi Bel Abbés, Algeria*
[5]*Département des Sciences et de la Technologie, Université de Tissemsilt, BP 38004 Ben Hamouda, Algérie*
[6]*Department of Mathematics, Govt. College University Faisalabad, 38000, Faisalabad, Pakistan*
[7]*YFL (Yonsei Frontier Lab), Yonsei University, Seoul, Korea*
[8]*Department of Civil and Environmental Engineering, King Fahd University of Petroleum & Minerals, Dhahran, Saudi Arabia*
[9]*Interdisciplinary Research Center for Construction and Building Materials, KFUPM, Dhahran, Saudi Arabia*

(Received June 26, 2020, Revised November 16, 2021, Accepted December 1, 2021)

Abstract. In this work, the bending and dynamic behaviors of advanced composite plates resting on variable visco-Pasternak foundations are studied using a simple shear deformation integral plate model. The research is carried out with a view to a three-parameter foundation including the influences of the variable Winkler coefficient, the constant Pasternak coefficient and the damping coefficient of the elastic medium. The present theory uses a displacement field with integral terms instead of derivative terms by including also the shear deformation effect without introducing the shear correction factors. The equations of motion for advanced composite plates are obtained using the Hamilton principle. Analytical solutions for the bending and dynamic analysis are deduced for simply supported plates resting on variable visco-Pasternak foundations. Some numerical results are presented to demonstrate the impact of material index, elastic foundation type, and damping coefficient of the foundation, on the bending and dynamic responses of advanced composite plates.

Keywords: bending; FGM; HSDT; Plate; variable visco-Pasternak foundations; vibration

1. Introduction

Functionally graded materials (FGMs) are microscopically inhomogeneous composites often fabricated from a mixture of ceramics and metals. By gradually varying the volume fraction of the constituent materials, the properties of the materials change progressively from one surface to another, thus eliminating the interface problems and attenuating the thermal stress concentrations in the composite materials. The concept of FGM has been widely employed in various engineering industries including civil, mechanics, aerospace, automotive, chemistry, optics, biomedicine, etc. (Koizumi 1997, Reddy 2000, Qian and Batra 2005, Akbaş 2015, Kar and Panda 2015, Kolahchi *et al.* 2016, Avcar 2019, Madenci 2019, Ahmed *et al.* 2019, Karami and Karami 2019, Akgün and Kurtaran 2019, Rachedi *et al.* 2020, Abdulrazzaq *et al.* 2020, Abdelrahman 2020, Shahmohammadi *et al.* 2020, Sadoughifar *et al.* 2020, Dehshahri *et al.* 2020, Fenjan *et al.* 2020a, Noroozi *et al.* 2020, Selmi 2020, Wang *et al.* 2020, Karakoti *et al.* 2021, Ebrahimi *et al.* 2021).

To mathematically examine the interaction between the plate and the foundation, several foundation models have been developed. The easiest is the one-parameter model often known by the Winkler model (Winkler 1867), which considers the foundations as a series of separate springs without coupling influences between them. Pasternak (1954) improved this model by adding a shear spring to simulate the interactions between separate springs in the Winkler model. Another improvement is assured by the visco-Pasternak model that is considered by adding the damping influence to the usual foundation model which characterized by the linear Winkler's modulus and Pasternak's (shear) foundation modulus.

Since the "shear deformation" influence is more remarked in FGMs, shear deformation theories should be employed to study functionally graded (FG) structures. The "first-order shear deformation theory" (FSDT) proposed by Mindlin (1951) and Reissner (1945) explains the effect of transverse shear deformation, but violates the "traction-free boundary conditions" on the upper and lower surfaces. A shear correction factor is therefore necessary to compensate for the difference between the actual state of stress and the considered constant stress state (Hosseini-Hashemi *et al.* 2010, Fallah *et al.* 2013). To avoid the use of this factor and to predict well the transverse shear deformation and normal

*Corresponding author, Ph.D.
E-mail: tounsi_abdeldjebbar@yahoo.com

ISSN: 2005-307X (Print), 2092-6219 (Online)

deformations in FG and composites plates, higher order shear deformation plate theories (HSDTs) have been developed. In general, HSDTs can be proposed on the basis of higher order variations of the in-plane displacements (Reddy 2000, Ferreira *et al.* 2005, Thai and Choi 2011, Xiang *et al*. 2011, Mantari *et al.* 2012, Xiang and Kang 2013, Sobhy 2013, Hirwani *et al.* 2017a, Hirwani *et al.* 2018a, b, Katariya *et al*. 2019, Katariya and Panda 2019a, Patle *et al*. 2020) or in-plane and transverse displacements (Chen *et al*. 2009, Fares *et al.* 2009, Talha and Singh 2010, Ferreira *et al*. 2011, Reddy 2011, Natarajan and Manickam 2012, Mantari and Guedes Soares 2012, 2013, Neves *et al.* 2012a, b, 2013, Thai and Kim 2013, Jha *et al.* 2013, Katariya and Panda 2019b, Karami and Janghorban 2019, Hirwani and Panda 2019a, b, Katariya *et al*. 2020) (i.e., quasi-3D theories). Also others HSDTs and Quasi-3D theories are developed and used in analytical studies and experimental validations to examine the static and dynamic behaviors of structures (Hirwani *et al*. 2017b, Hirwani and Panda 2018, Hirwani *et al*. 2018c, d, e, Sahoo *et al*. 2019, Singh *et al.* 2019, Pandey *et al*. 2020). However, HSDTs represent a high computational cost because of their involvement in many unknowns (for example, the theories of Neves *et al*. (2012a, b, 2013) with nine unknowns, Reddy (2011) with eleven unknowns, Jha *et al*. (2013) with twelve unknowns, Talha and Singh (2010) and Natarajan and Manickam (2012) with thirteen unknowns). Thus, a simple HSDT proposed in this work is necessary.

This work aims to develop a simple shear deformation integral plate theory for bending and free vibration analysis of FG plates located on a variable visco-Pasternak elastic foundation. Hamilton's principle is employed to derive motion equations and Navier-type analytical solutions for simply-supported FG plates are compared with the existing solutions to check the validity of the proposed theory. The results of current research will help improve the prediction of the mechanical behavior of structures and design them to achieve the desired results.

2. Theoretical formulations

2.1 FG-plate properties

In the present investigation, a rectangular simply supported FG plate seated on visco-Pasternak foundations is considered (see Fig.1). The studied plate occupies the regions $[0,a]\times[0,b]\times[-h/2,h/2]$ in the Cartesian coordinate system. Two type of material are used to made the FG plate which the properties P(z) vary according to power law function as follow

$$P(z)=P_M+\left(P_C-P_M\right)\left(\frac{2z+h}{2h}\right)^p \tag{1}$$

Where the subscripts C and M represent the ceramic and metallic constituents, respectively. P is the effective material property like mass density ρ and Young's modulus

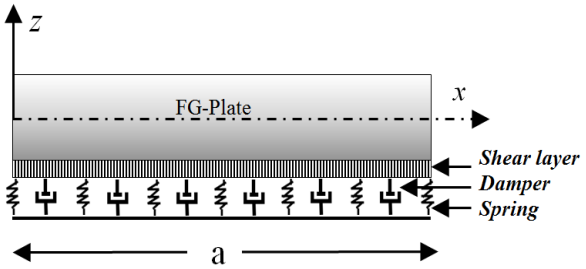

Fig. 1 The scheme of FG plate resting on visco-Pasternak elastic foundation

E and p is the material index.

2.2 Shear deformation integral plate theory

Based on the higher order shear deformation theory assumptions, after certain modifications and simplifications. The present shear deformation integral plate model take the following form

$$\begin{aligned} u(x,y,z)&=u_0(x,y)-z\frac{\partial w_0(x,y)}{\partial x}+k_1 f(z)\int\theta(x,y)dx\\ v(x,y,z)&=v_0(x,y)-z\frac{\partial w_0(x,y)}{\partial y}+k_2 f(z)\int\theta(x,y)dy\\ w(x,y,z)&=w_0(x,y)\end{aligned} \tag{2}$$

The deformation field associated to the above displacement field is obtained as

$$\begin{Bmatrix}\varepsilon_x\\ \varepsilon_y\\ \varepsilon_{xy}\end{Bmatrix}=\begin{Bmatrix}\varepsilon_x^0\\ \varepsilon_y^0\\ \varepsilon_{xy}^0\end{Bmatrix}+z\begin{Bmatrix}\varepsilon_x^1\\ \varepsilon_y^1\\ \varepsilon_{xy}^1\end{Bmatrix}+f(z)\begin{Bmatrix}\varepsilon_x^2\\ \varepsilon_y^2\\ \varepsilon_{xy}^2\end{Bmatrix},\quad\begin{Bmatrix}\gamma_{xz}\\ \gamma_{yz}\end{Bmatrix}=g(z)\begin{Bmatrix}\gamma_{xz}^0\\ \gamma_{yz}^0\end{Bmatrix} \tag{3}$$

where

$$\begin{Bmatrix}\varepsilon_x^0\\ \varepsilon_y^0\\ \varepsilon_{xy}^0\end{Bmatrix}=\begin{Bmatrix}\dfrac{\partial u_0}{\partial x}\\ \dfrac{\partial v_0}{\partial y}\\ \dfrac{\partial u_0}{\partial y}+\dfrac{\partial v_0}{\partial x}\end{Bmatrix},\quad\begin{Bmatrix}\varepsilon_x^1\\ \varepsilon_y^1\\ \varepsilon_{xy}^1\end{Bmatrix}=\begin{Bmatrix}-\dfrac{\partial^2 w_0}{\partial x^2}\\ -\dfrac{\partial^2 w_0}{\partial y^2}\\ -2\dfrac{\partial^2 w_0}{\partial x\partial y}\end{Bmatrix}, \tag{4a}$$

$$\begin{Bmatrix}\gamma_{xz}^0\\ \gamma_{yz}^0\end{Bmatrix}=\begin{Bmatrix}K_1\int\theta(x,y)dx\\ K_2\int\theta(x,y)dy\end{Bmatrix}$$

$$\begin{Bmatrix}\varepsilon_x^2\\ \varepsilon_y^2\\ \varepsilon_{xy}^2\end{Bmatrix}=\begin{Bmatrix}K_1\theta(x,y)\\ K_2\theta(x,y)\\ K_1\dfrac{\partial}{\partial y}\int\theta(x,y)dx+K_2\dfrac{\partial}{\partial x}\int\theta(x,y)dy\end{Bmatrix} \tag{4b}$$

$$f(z)=\frac{h}{\pi}\sin\left(\frac{\pi z}{h}\right)\qquad g(z)=\frac{\partial f(z)}{\partial z} \tag{4c}$$

In this investigation, the integrals appearing in the above expressions of the current model shall be resolved by a Navier type solution and can be obtained as follows

$$\frac{\partial}{\partial y}\int \theta dx = A^{'}\frac{\partial^2\theta}{\partial x\partial y};\ \frac{\partial}{\partial x}\int \theta dy = B^{'}\frac{\partial^2\theta}{\partial x\partial y}$$
$$\int \theta dx = A^{'}\frac{\partial\theta}{\partial x};\ \int \theta dy = B^{'}\frac{\partial\theta}{\partial y} \tag{5}$$

With

$$A^{'} = -\frac{1}{\alpha^2}, B^{'} = -\frac{1}{\beta^2}, k_1 = \alpha^2, k_2 = \beta^2 \tag{6}$$

where "$A^{'}$" and "$B^{'}$" are the coefficients defined according to the type of solution adopted.

The constitutive relations (stress-strain) of the P-FG plate can be written as

$$\begin{Bmatrix}\sigma_x\\ \sigma_y\\ \tau_{yz}\\ \tau_{xz}\\ \tau_{xy}\end{Bmatrix} = \begin{bmatrix} Q_{11} & Q_{12} & 0 & 0 & 0\\ Q_{21} & Q_{22} & 0 & 0 & 0\\ 0 & 0 & Q_{44} & 0 & 0\\ 0 & 0 & 0 & Q_{55} & 0\\ 0 & 0 & 0 & 0 & Q66\end{bmatrix}\begin{Bmatrix}\begin{Bmatrix}\varepsilon_x\\ \varepsilon_y\\ \gamma_{yz}\\ \gamma_{xz}\\ \gamma_{xy}\end{Bmatrix}\end{Bmatrix} \tag{7}$$

where "σ,τ" and "ε,γ" are stresses and strains , respectively. The elastic stiffness's $Q_{ij}(i,j=1,2,4,5,6)$ are given by:

$$Q_{11} = Q_{22} = \frac{E(z)}{1-\upsilon^2} \qquad Q_{12} = Q_{21} = \frac{\upsilon E(z)}{1-\upsilon^2}$$
$$Q_{44} = Q_{55} = Q_{66} = \frac{E(z)}{2(1+\upsilon)} \tag{8}$$

Where "$E(z)$" is the Young modulus and "ν" is the Poison's ratio

2.3 equations of motion

In this work, the equations of motion are determined based on the following Hamilton's principle.

$$\int_0^t \delta\left(U + U_F - V + K\right)dt = 0, \tag{9}$$

Where U is the strain energy, U_F is the strain energy induced by the elastic foundations, *V is the* work of external (applied) forces and K is the kinetic energy.

Based on the current formulation, the variation of strain energy U can be written as

$$\delta U = \int_A\int_{-h/2}^{h/2}\left(\sigma_x\delta\varepsilon_x + \sigma_y\delta\varepsilon_y + \tau_{xy}\delta\gamma_{xy} + \tau_{xz}\delta\gamma_{xz} + \tau_{yz}\delta\gamma_{yz}\right)dAdz$$
$$= \int_A\Big[N_x\delta\ \varepsilon_x^0 + N_{xy}\delta\gamma_{xy}^0 + N_y\delta\ \varepsilon_y^0 + M_x\delta\ \varepsilon_x^1 + M_y\delta\ \varepsilon_y^1 \tag{10a}$$
$$+M_{xy}\delta\ \varepsilon_{xy}^1 + S_x\delta\ \varepsilon_x^2 + S_y\delta\ \varepsilon_y^2 + S_{xy}\delta\ \varepsilon_{xy}^2 + Q_{yz}\delta\gamma_{yz}^0 + Q_{xz}\delta\gamma_{xz}^0\Big]dA$$

where A is the top surface.

The strain energy U_F induced by elastic foundations can be defined as

$$\delta U_F = \int_A R(x)\delta w_0 dA \tag{10b}$$

The variation of work δV done by transverse load q can be expressed as

$$\delta V = -\int_A q(x,y)\delta w_0 dA \tag{10c}$$

The variation of kinetic energy δK is expressed as

$$\delta\ K = \int_V\left[\dot{u}\,\delta\ \dot{u} + \dot{v}\,\delta\ \dot{v} + \dot{w}\delta\ \dot{w}\right]\ \rho(z)\ dV$$
$$= \int_A\{I_1\left[\dot{u}_0\delta\dot{u}_0 + \dot{v}_0\delta\dot{v}_0 + \dot{w}_0\delta\dot{w}_0\right]$$
$$-I_2\left(\dot{u}_0\frac{\partial\delta\dot{w}_0}{\partial x} + \frac{\partial\dot{w}_0}{\partial x}\delta\ \dot{u}_0 + \dot{v}_0\frac{\partial\delta\dot{w}_0}{\partial y} + \frac{\partial\dot{w}_0}{\partial y}\delta\ \dot{v}_0\right)$$
$$+I_4\left(\left(k_1\,A^{'}\right)\left(\dot{u}_0\frac{\partial\delta\dot{\theta}}{\partial x} + \frac{\partial\dot{\theta}}{\partial x}\delta\ \dot{u}_0\right) + \left(k_2\,B^{'}\right)\left(\dot{v}_0\frac{\partial\delta\dot{\theta}}{\partial y} + \frac{\partial\dot{\theta}}{\partial y}\delta\ \dot{v}_0\right)\right)$$
$$+I_3\left(\frac{\partial\dot{w}_0}{\partial x}\frac{\partial\delta\ \dot{w}_0}{\partial x} + \frac{\partial\dot{w}_0}{\partial y}\frac{\partial\delta\ \dot{w}_0}{\partial y}\right) \tag{10d}$$
$$+I_6\left(\left(k_1\,A^{'}\right)^2\left(\frac{\partial\dot{\theta}}{\partial x}\frac{\partial\delta\ \dot{\theta}}{\partial x}\right) + \left(k_2\,B^{'}\right)^2\left(\frac{\partial\dot{\theta}}{\partial y}\frac{\partial\delta\ \dot{\theta}}{\partial y}\right)\right)$$
$$-I_5\left(\left(k_1\,A^{'}\right)\left(\frac{\partial\dot{w}_0}{\partial x}\frac{\partial\delta\ \dot{\theta}}{\partial x} + \frac{\partial\dot{\theta}}{\partial x}\frac{\partial\delta\ \dot{w}_0}{\partial x}\right)\right.$$
$$\left.+\left(k_2\,B^{'}\right)\left(\frac{\partial\dot{w}_0}{\partial y}\frac{\partial\delta\ \dot{\theta}}{\partial y} + \frac{\partial\dot{\theta}}{\partial y}\frac{\partial\delta\ \dot{w}_0}{\partial y}\right)\right)\Big\}dA$$

By substituting the Eqs. (10) into Hamilton's principle of Eq. (9), integrating by part and separation the terms of displacement, The four equations of motion associated to the current analytical model of the P-FG plate resting visco-elastic foundation are obtained as

$$\delta\ u_0: \quad \frac{\partial N_x}{\partial x} + \frac{\partial N_{xy}}{\partial y} = I_1\ddot{u}_0 - I_2\ddot{w}_{0,x} + I_4k_1\,A^{'}\ddot{\theta}_{,x} \tag{11a}$$

$$\delta\ v_0: \quad \frac{\partial N_{xy}}{\partial x} + \frac{\partial N_y}{\partial y} = I_1\ddot{v}_0 - I_2\ddot{w}_{0,y} + I_4k_2\ B^{'}\ddot{\theta}_{,y} \tag{11b}$$

$$\delta\ w_0: \quad \frac{\partial^2 M_x}{\partial x^2} + \frac{\partial^2 M_y}{\partial y^2} + 2\frac{\partial^2 M_{xy}}{\partial x\partial y} - R(x) - q(x,y)$$
$$= I_1\ddot{w}_0 + I_2\left(\ddot{u}_{0,x} + \ddot{v}_{0,y}\right) - I_3\left(\ddot{w}_{0,xx} + \ddot{w}_{0,yy}\right) \tag{11c}$$
$$+I_5\left(k_1\,A^{'}\ddot{\theta}_{,xx} + k_2\ B^{'}\ddot{\theta}_{,yy}\right)$$

$$\delta\ \theta: \ -k_1\,A^{'}\frac{\partial^2 S_x}{\partial x^2} - k_2\ B^{'}\frac{\partial^2 S_y}{\partial y^2} - \left(k_1\,A^{'} + k_2B^{'}\right)\frac{\partial^2 S_{xy}}{\partial x\partial y}$$
$$+k_1\,A^{'}\frac{\partial Q_{xz}}{\partial x} + k_2B^{'}\frac{\partial Q_{yz}}{\partial y} = -I_4\left(k_1\,A^{'}\ddot{u}_{0,x} + k_2\ B^{'}\ddot{v}_{0,y}\right) \tag{11d}$$
$$+I_5\left(k_1\,A^{'}\ddot{w}_{0,xx} + k_2\ B^{'}\ddot{w}_{0,yy}\right) - I_6\left(k_1^{\ 2}\,A^{'2}\ddot{\theta}_{,xx} + k_2^{\ 2}\ B^{'2}\ddot{\theta}_{,yy}\right)$$

Where the terms $N, M, S\ and\ Q$ are the stress and moment resultants, $q(x,y)$ is transversal mechanical load, I_i is the mass inertia and $R(x)$ is the response of the visco-elastic foundation parameter defined by

$$R\left(x\right) = k_w\left(x\right)w_0 - k_s\nabla^2 w_0 + ct\,\dot{w}_0 \tag{12a}$$

Where $k_w, k_s\ and\ ct$ are the Winkler parameters, shear layer and damping constants, respectively. In this work the Winkler parameter is in function of x only. Three types of variation are assumed (Pradhan and Murmu 2009)

$$K_w(x) = \frac{\bar{k}_w h^3}{a^4}\begin{cases}1 + \xi\left(\frac{x}{a}\right) & Linear\\ 1 + \xi\left(\frac{x}{a}\right)^2 & Parabolic\\ 1 + \xi sin\left(\frac{\pi x}{a}\right) & sinusiodal\end{cases} \tag{12b}$$

In this case, if the parameter $k_w = 0$ the plate is reposed on Pasternak foundation and if shear layer parameter $k_s = 0$ is neglected, the elastic foundation becomes the Winkler foundation.

The stress and moment resultants $N, M, S \text{ and } Q$ are defined as

$$\begin{Bmatrix} N_x & N_y & N_{xy} \\ M_x & M_y & M_{xy} \\ S_x & S_y & S_{xy} \end{Bmatrix} = \int_{-\frac{h}{2}}^{\frac{h}{2}} \left(\sigma_x, \sigma_y, \tau_{xy}\right) \begin{Bmatrix} 1 \\ z \\ f(z) \end{Bmatrix} dz \tag{13a}$$

$$\left(Q_{xz}, Q_{yz}\right) = \int_{-\frac{h}{2}}^{\frac{h}{2}} \left(\tau_{xz}, \tau_{yz}\right) g(z) dz \tag{13b}$$

The terms of mass inertia $I_1, I_2, I_3, I_4, I_5 \text{ and } I_6$ are defined as

$$I_1, I_2, I_3, I_4, I_5, I_6 = \int_{-\frac{h}{2}}^{\frac{h}{2}} \rho(z)\left(1, z, z^2, f(z), zf(z), \left[f(z)\right]^2\right) dz \tag{14}$$

By substituting the Eq. (7) into (13), the resultants forces and moment are obtained as

$$\begin{Bmatrix} N_x \\ N_y \\ N_{xy} \\ M_x \\ M_y \\ M_{xy} \\ S_x \\ S_y \\ S_{xy} \end{Bmatrix} = \begin{bmatrix} A_{11} & A_{12} & 0 & B_{11} & B_{12} & 0 & B^s_{11} & B^s_{12} & 0 \\ A_{12} & A_{22} & 0 & B_{12} & B_{22} & 0 & B^s_{12} & B^s_{22} & 0 \\ 0 & 0 & A_{66} & 0 & 0 & B_{66} & 0 & 0 & B^s_{66} \\ B_{11} & B_{12} & 0 & D_{11} & D_{12} & 0 & D^s_{11} & D^s_{12} & 0 \\ B_{12} & B_{22} & 0 & D_{12} & D_{22} & 0 & D^s_{12} & D^s_{22} & 0 \\ 0 & 0 & B_{66} & 0 & 0 & D_{66} & 0 & 0 & D^s_{66} \\ B^s_{11} & B^s_{12} & 0 & D^s_{11} & D^s_{12} & 0 & H^s_{11} & H^s_{12} & 0 \\ B^s_{12} & B^s_{22} & 0 & D^s_{12} & D^s_{22} & 0 & H^s_{12} & H^s_{22} & 0 \\ 0 & 0 & B^s_{66} & 0 & 0 & D^s_{66} & 0 & 0 & H^s_{66} \end{bmatrix} \begin{Bmatrix} \varepsilon^0_x \\ \varepsilon^0_y \\ \varepsilon^0_{xy} \\ \varepsilon^1_x \\ \varepsilon^1_y \\ \varepsilon^1_{xy} \\ \varepsilon^2_x \\ \varepsilon^2_y \\ \varepsilon^2_{xy} \end{Bmatrix} \tag{15a}$$

$$\begin{Bmatrix} Q_{yz} \\ Q_{xz} \end{Bmatrix} = \begin{bmatrix} A^s_{44} & 0 \\ 0 & A^s_{55} \end{bmatrix} \begin{Bmatrix} \gamma^0_{yz} \\ \gamma^0_{xz} \end{Bmatrix} \tag{15b}$$

where $A_{ij}, B_{ij}, D_{ij}, H_{ij}$,are the plate stiffness, defined by

$$\begin{Bmatrix} A_{11} & B_{11} & D_{11} & B^s_{11} & D^s_{11} & H^s_{11} \\ A_{12} & B_{12} & D_{12} & B^s_{12} & D^s_{12} & H^s_{12} \\ A_{66} & B_{66} & D_{66} & B^s_{66} & D^s_{66} & H^s_{66} \end{Bmatrix} = \int_{-\frac{h}{2}}^{\frac{h}{2}} Q_{11}\left(1, z, z^2, f(z), zf(z), f^2(z)\right) \begin{Bmatrix} 1 \\ \upsilon \\ \frac{1-\upsilon}{2} \end{Bmatrix} dz \tag{16a}$$

$$\left(A_{22}, B_{22}, D_{22}, B^s_{22}, D^s_{22}, H^s_{22}\right) = \left(A_{11}, B_{11}, D_{11}, B^s_{11}, D^s_{11}, H^s_{11}\right) \tag{16b}$$

$$A^s_{44} = A^s_{55} = \int_{-\frac{h}{2}}^{\frac{h}{2}} \frac{E(z)}{2(1+\upsilon)} \left[g(z)\right]^2 dz \tag{16c}$$

Substituting Eq. (4) and Eq. (15) into Eqs. (11), the equation of motion are obtained in function of the displacement terms ($u_0, v_0, w_0 \text{ and } \theta$) as

$$\begin{aligned} &A_{11}\frac{\partial^2 u_0}{\partial x^2} + A_{12}\frac{\partial^2 v_0}{\partial x \partial y} + A_{66}\left(\frac{\partial^2 u_0}{\partial y^2} + \frac{\partial^2 v_0}{\partial x \partial y}\right) - B_{11}\frac{\partial^3 w_0}{\partial x^3} \\ &-B_{12}\frac{\partial^3 w_0}{\partial x \partial y^2} - 2B_{66}\frac{\partial^3 w_0}{\partial x \partial y^2} + B^s_{11}A'k_1\frac{\partial^3 \theta}{\partial x^3} B^s_{12}B'k_2\frac{\partial^3 \theta}{\partial x \partial y^2} \\ &+B^s_{66}\left(A'k_1 + B'k_2\right)\frac{\partial^3 \theta}{\partial x \partial y^2} - I_1\ddot{u}_0 + I_2\ddot{w}_{0,x} - I_4 k_1\, A'\ddot{\theta}_{,x} = 0 \end{aligned}$$

$$\begin{aligned} &A_{12}\frac{\partial^2 u_0}{\partial x \partial y} + A_{22}\frac{\partial^2 v_0}{\partial y^2} + A_{66}\left(\frac{\partial^2 u_0}{\partial x \partial y} + \frac{\partial^2 v_0}{\partial x^2}\right) - B_{12}\frac{\partial^3 w_0}{\partial x^2 \partial y} \\ &-B_{22}\frac{\partial^3 w_0}{\partial y^3} - 2B_{66}\frac{\partial^3 w_0}{\partial x^2 \partial y} + B^s_{12}A'k_1\frac{\partial^3 \theta}{\partial x^2 \partial y} B^s_{22}B'k_2\frac{\partial^3 \theta}{\partial y^3} \\ &+B^s_{66}\left(A'k_1 + B'k_2\right)\frac{\partial^3 \theta}{\partial x^2 \partial y} - I_1\ddot{v}_0 + I_2\ddot{w}_{0,y} - I_4 k_2\, B'\ddot{\theta}_{,y} = 0 \end{aligned} \tag{17a}$$

$$B_{11}\left(\frac{\partial^3 u_0}{\partial x^3}\right) + B_{12}\left(\frac{\partial^3 u_0}{\partial x \partial y^2} + \frac{\partial^3 v_0}{\partial x^2 \partial y}\right) + B_{22}\left(\frac{\partial^3 v_0}{\partial y^3}\right) \tag{17b}$$

$$\begin{aligned} &+2B_{66}\left(\frac{\partial^3 u_0}{\partial x \partial y^2} + \frac{\partial^3 v_0}{\partial x^2 \partial y}\right) - D_{11}\left(\frac{\partial^4 w_0}{\partial x^4}\right) - 2D_{12}\left(\frac{\partial^4 w_0}{\partial x^2 \partial y^2}\right) \\ &-D_{22}\left(\frac{\partial^4 w_0}{\partial y^4}\right) - 4D_{66}\left(\frac{\partial^4 w_0}{\partial x^2 \partial y^2}\right) + D^s_{11}A'k_1\left(\frac{\partial^4 \theta}{\partial x^4}\right) \\ &+D^s_{12}\left(A'k_1 + B'k_2\right)\frac{\partial^4 \theta}{\partial x^2 \partial y^2} + D^s_{22}B'k_2\left(\frac{\partial^4 \theta}{\partial y^4}\right) \\ &+2D^s_{66}\left(A'k_1 + B'k_2\right)\left(\frac{\partial^4 \theta}{\partial x^2 \partial y^2}\right) - K_w(x)w_0 \\ &+K_s\left(\frac{\partial^2 w_0}{\partial x^2} + \frac{\partial^2 w_0}{\partial y^2}\right) - ct\left(\frac{\partial\, w_0}{\partial x}\right) - I_1\ddot{w}_0 - I_2\left(\ddot{u}_{0,x} + \ddot{v}_{0,y}\right) \\ &+I_3\left(\ddot{w}_{0,xx} + \ddot{w}_{0,yy}\right) - I_5\left(k_1\, A'\ddot{\theta}_{,xx} + k_2\, B'\ddot{\theta}_{,yy}\right) = 0 \end{aligned} \tag{17c}$$

$$\begin{aligned} &-B^s_{11}A'k_1\left(\frac{\partial^3 u_0}{\partial x^3}\right) - B^s_{12}\left(A'k_1\frac{\partial^3 v_0}{\partial x^2 \partial y} + B'k_2\frac{\partial^3 u_0}{\partial x \partial y^2}\right) \\ &-B^s_{22}B'k_2\left(\frac{\partial^3 v_0}{\partial y^3}\right) - D_{66}\left(\left(A'k_1 + B'k_2\right)\frac{\partial^3 u_0}{\partial x \partial y^2}\right. \\ &\left.+\left(A'k_1 + B'k_2\right)\frac{\partial^3 v_0}{\partial x^2 \partial y}\right) + D^s_{11}A'k_1\frac{\partial^4 w_0}{\partial x^4} \\ &+D^s_{12}\left(A'k_1 + B'k_2\right)\frac{\partial^4 w_0}{\partial x^2 \partial y} D^s_{22}B'k_2\frac{\partial^4 w_0}{\partial y^4} \\ &+2D^s_{66}\left(A'k_1 + B'k_2\right)\frac{\partial^4 w_0}{\partial x^2 \partial y} - H^s_{11}\left(A'k_1\right)^2\frac{\partial^4 \theta}{\partial x^4} \\ &-2H^s_{12}A'k_1B'k_2\frac{\partial^4 \theta}{\partial x^2 \partial y^2} - H^s_{22}\left(B'k_2\right)^2\frac{\partial^4 \theta}{\partial y^4} \\ &-H^s_{66}\left(A'k_1 + B'k_2\right)^2\left(\frac{\partial^4 \theta}{\partial x^2 \partial y}\right) + A^s_{55}\left(A'k_1\right)^2\left(\frac{\partial^2 \theta}{\partial x?}\right) \\ &+A^s_{44}\left(B'k_2\right)^2\left(\frac{\partial^2 \theta}{\partial y^2}\right) + I_4\left(k_1\, A'\ddot{u}_{0,x} + k_2\, B'\ddot{v}_{0,y}\right) \\ &-I_5\left(k_1\, A'\ddot{w}_{0,xx} + k_2\, B'\ddot{w}_{0,yy}\right) \\ &+I_6\left(k_1^2\, A'^2\ddot{\theta}_{,xx} + k_2^2\, B'^2\ddot{\theta}_{,yy}\right) = 0 \end{aligned} \tag{17d}$$

2.4 Closed-form solution:

For the simply supported P-FG plate modeled via four variable integral shear deformation theory, the four equation of motion are solved by the Navier method which the displacements u_0, v_0, w_0, θ are chosen to automatically satisfy the boundary conditions.

$$\begin{Bmatrix} u_0 \\ v_0 \\ w_0 \\ \theta \end{Bmatrix} = \sum_{m=1}^{\infty}\sum_{n=1}^{\infty} \begin{Bmatrix} U_{mn}\cos(\lambda x)\sin(\mu y)e^{i\omega t} \\ V_{mn}\sin(\lambda x)\cos(\mu y)e^{i\omega t} \\ W_{mn}\sin(\lambda x)\sin(\mu y)e^{i\omega t} \\ \theta_{mn}\sin(\lambda x)\sin(\mu y)e^{i\omega t} \end{Bmatrix}, \tag{18}$$

With

$$\lambda = m\pi/a\,, \quad \mu = n\pi/b \tag{19}$$

Where $U_{mn}, V_{mn}, W_{mn}, \theta_{mn}$ are arbitrary parameters to be determined. m , n are the mode numbers, and $i = \sqrt{-1}$.

The transverse mechanical load $q(x,y)$ is also expanded in the double-Fourier sine series as

$$q(x,y) = \sum_{m=1}^{\infty}\sum_{n=1}^{\infty} Q_{mn} \sin\ \lambda x\ \sin\ \mu y \tag{20}$$

With

$$Q_{mn} = \frac{4}{ab}\int_0^a\int_0^b q(x,y)\sin\lambda x \sin\mu y\, dxdy = \begin{cases} q_0 e_3 & \text{for sinusoidal load} \\ \dfrac{16q_0}{mn\pi^2}e_3 & \text{for uniform load} \end{cases} \tag{21}$$

Substituting the Eq. (18) into Eq. (17). We obtain the following matrix system:

$$\left([K]-\omega^2[M]\right)\{\Delta\} = \{0\} \tag{22}$$

Where [K] and [M], stiffness and mass matrices, respectively, with

$$[K] = \begin{bmatrix} a_{11} & a_{12} & a_{13} & a_{14} \\ a_{12} & a_{22} & a_{23} & a_{24} \\ a_{13} & a_{23} & a_{33} & a_{34} \\ a_{14} & a_{24} & a_{34} & a_{44} \end{bmatrix} \quad \{\Delta\} = \begin{Bmatrix} U_{mn} \\ V_{mn} \\ W_{mn} \\ \theta_{mn} \end{Bmatrix} \tag{23a}$$

$$[M] = \begin{bmatrix} m_{11} & m_{12} & m_{13} & m_{14} \\ m_{12} & m_{22} & m_{23} & m_{24} \\ m_{13} & m_{23} & m_{33} & m_{34} \\ m_{14} & m_{24} & m_{34} & m_{44} \end{bmatrix} \tag{23b}$$

In which

$$\begin{aligned} a_{11} &= \left(-(A_{11}\lambda^2 + A_{66}\mu^2)\right)e_1 \\ a_{12} &= \left(-\lambda\ \mu\ \left(A_{12}+A_{66}\right)\right)e_1 \\ a_{13} &= \left(\lambda(B_{11}\lambda^2 + (B_{12}+2B_{66})\mu^2)\right)e_1 \\ a_{14} &= -\lambda(B^s_{11}A'k_1\lambda^2 + B^s_{12}B'k_2\mu^2 + B^s_{66}\left(A'k_1 + B'k_2\right)\mu^2) \end{aligned} \tag{24a}$$

$$\begin{aligned} a_{21} &= \left(-\lambda\ \mu\ \left(A_{12}+A_{66}\right)\right)e_2 \\ a_{22} &= -\lambda^2 A_{66} - \mu^2 A_{22} \\ a_{23} &= \left(\mu(B_{22}\mu^2 + (B_{12}+2B_{66})\lambda^2)\right)e_2 \\ a_{24} &= \left(-\mu\left(B^s_{22}B'k_2\mu^2 + \lambda^2\left(B^s_{12}A'k_1 + B^s_{66}\left(A'k_1 + B'k_2\right)\right)\right)\right)e_2 \\ a_{31} &= \left(\lambda(B_{11}\lambda^2 + (B_{12}+2B_{66})\mu^2)\right)e_3 \\ a_{32} &= \left(\mu(B_{22}\mu^2 + (B_{12}+2B_{66})\lambda^2)\right)e_3 \\ a_{33} &= \begin{pmatrix} -\lambda^2\left(D_{11}\lambda^2 + \left(2D_{12}+4D_{66}\right)\mu^2\right) - D_{22}\mu^4 \\ -K_s\left(\lambda^2+\mu^2\right) - \mathrm{ct}*\omega \end{pmatrix} e_3 - e_4 \\ a_{34} &= \begin{pmatrix} D^s_{11}A'k_1\lambda^4 + D^s_{12}\left(A'k_1 + B'k_2\right)\mu^2\lambda^2 + D^s_{22}B'k_2\mu^4 \\ +2D^s_{66}\left(A'k_1 + B'k_2\right)\mu^2\lambda^2 \end{pmatrix} e_3 \\ a_{41} &= \left(-\lambda(B^s_{11}A'k_1\lambda^2 + B^s_{12}B'k_2\mu^2 + B^s_{66}\left(A'k_1 + B'k_2\right)\mu^2)\right)e_3 \\ a_{42} &= \left(-\mu\left(B^s_{22}B'k_2\mu^2 + \lambda^2\left(B^s_{12}A'k_1 + B^s_{66}\left(A'k_1 + B'k_2\right)\right)\right)\right)e_3 \\ a_{43} &= \begin{pmatrix} D^s_{11}A'k_1\lambda^4 + D^s_{12}\left(A'k_1 + B'k_2\right)\mu^2\lambda^2 + D^s_{22}B'k_2\mu^4 \\ +2D^s_{66}\left(A'k_1 + B'k_2\right)\mu^2\lambda^2 \end{pmatrix} e_3 \\ a_{44} &= \begin{pmatrix} -H^s_{11}\left(A'k_1\right)^2\lambda^4 - 2H^s_{12}A'k_1B'k_2\lambda^2\mu^2 - H^s_{22}\left(B'k_2\right)^2\mu^4 \\ -H^s_{66}\left(A'k_1 + B'k_2\right)^2\lambda^2\mu^2 - A^s_{55}\left(A'k_1\right)^2\lambda^2 - A^s_{44}\left(B'k_2\right)^2\mu^2 \end{pmatrix} e_3 \end{aligned}$$

$$\begin{aligned} m_{11} &= -I_1 e_1 \\ m_{12} &= 0 \\ m_{13} &= I_2\lambda\ e_1 \\ m_{14} &= -I_4 K_1 A'\lambda\ e_1 \\ m_{21} &= 0 \\ m_{22} &= -I_1 e_2 \\ m_{23} &= I_2\mu\ e_2 \\ m_{24} &= -I_4 K_2 B'\mu\ e_2 \\ m_{31} &= I_2\lambda\ e_3 \\ m_{32} &= I_2\mu\ e_3 \\ m_{33} &= (-I_3(\lambda^2+\mu^2) - I_1)e_3 \\ m_{34} &= \left(I_5(K_1A'\lambda^2 + K_2B'\mu^2)\right)e_3 \\ m_{41} &= -I_4 K_1 A'\lambda\ e_3 \\ m_{42} &= -I_4 K_2 B'\mu\ e_3 \\ m_{43} &= \left(I_5\left(K_1A'\lambda^2 + K_2B'\mu^2\right)\right)e_3 \\ m_{43} &= \left(-I_6\left({K_1}^2A'^2\lambda^2 + {K_2}^2B'^2\mu^2\right)\right)e_3 \end{aligned} \tag{24b}$$

$$e_1 = \int_0^a\int_0^b sin(\mu\ y)^2\, cos(\lambda\ x)^2 dy\ dx$$

$$e_2 = \int_0^a\int_0^b cos(\mu\ y)^2\, sin(\lambda\ x)^2 dy\ dx$$

$$e_3 = \int_0^a\int_0^b sin(\lambda\ x)^2\, sin(\mu\ y\ )^2 dy\ dx$$

$$e_4 = \int_0^a\int_0^b K_w(x)\ sin(\lambda\ x)^2\, sin(\mu\ y\ )^2 dy\ d$$

Table 1 Dimensionless deflection (w^*) and stresses (σ_x^*, σ_y^* and σ_{xy}^*) of rectangular plates under uniform loads ($a/h = 10, b = 3a$)

K_0	J_0	Method	p=0				p=0.5				p=1				p=2				p=5			
			w^*	σ_x^*	σ_y^*	σ_{xy}^*	w^*	σ_x^*	σ_y^*	σ_{xy}^*	w^*	σ_x^*	σ_y^*	σ_{xy}^*	w^*	σ_x^*	σ_y^*	σ_{xy}^*	w^*	σ_x^*	σ_y^*	σ_{xy}^*
0	0	SSDT [a]	1.2583	0.7162	0.2448	0.2893	1.9344	0.2337	0.0799	0.0941	2.5133	0.3250	0.1111	0.1307	3.2267	0.4396	0.1502	0.1766	3.8517	0.5224	0.1785	0.2104
		ZSDT[b]	1.2583	0.7160	0.2447	0.2890	1.9345	0.2337	0.0799	0.0941	2.5134	0.3250	0.1111	0.1306	3.2266	0.4395	0.1502	0.1766	3.8506	0.5223	0.1785	0.2103
		Present ct=0	1.2583	0.7161	0.2447	0.2895	1.9344	0.2337	0.0799	0.0942	2.5135	0.3250	0.1111	0.1308	3.2274	0.4396	0.1502	0.1767	3.8529	0.5225	0.1785	0.2106
		Present ct=0.01	1.2030	0.6834	0.2324	0.2810	1.8074	0.2178	0.0739	0.0900	2.3025	0.2967	0.1004	0.1234	2.8857	0.3913	0.1322	0.1641	3.3754	0.4552	0.1534	0.1929
		Present ct=0.02	1.1522	0.6533	0.2212	0.2730	1.6944	0.2036	0.0686	0.0863	2.1221	0.2724	0.0914	0.1169	2.6071	0.3519	0.1175	0.1535	2.9993	0.4023	0.1339	0.1786
		Present ct=0.1	0.8577	0.4794	0.1572	0.2256	1.1224	0.1319	0.0425	0.0663	1.2916	0.1612	0.0512	0.0854	1.4517	0.1892	0.0592	0.1063	1.5600	0.2008	0.0622	0.1189
100	0	SSDT [a]	1.2259	0.6970	0.2376	0.2843	1.8590	0.2242	0.0763	0.0916	2.3874	0.3081	0.1047	0.1263	3.0219	0.4106	0.1394	0.1690	3.5629	0.4816	0.1633	0.1997
		ZSDT[b]	1.2260	0.6969	0.2375	0.2840	1.8590	0.2242	0.0763	0.0916	2.3875	0.3080	0.1047	0.1262	3.0218	0.4105	0.1394	0.1690	3.5620	0.4816	0.1633	0.1996
		Present ct=0	1.2259	0.6969	0.2375	0.2845	1.8590	0.2242	0.0763	0.0917	2.3877	0.3081	0.1047	0.1264	3.0220	0.4105	0.1393	0.1691	3.5634	0.4816	0.1633	0.1999
		Present ct=0.01	1.1733	0.6658	0.2258	0.2763	1.7404	0.2093	0.0707	0.0878	2.1958	0.2823	0.0951	0.1196	2.7194	0.3678	0.1234	0.1578	3.1483	0.4233	0.1416	0.1843
		Present ct=0.02	1.1248	0.6371	0.2151	0.2687	1.6352	0.1961	0.0658	0.0843	2.0302	0.2601	0.0869	0.1136	2.4698	0.3325	0.1104	0.1482	2.8173	0.3767	0.1245	0.1715
		Present ct=0.1	0.8420	0.4702	0.1538	0.2230	1.0954	0.1286	0.0413	0.0653	1.2556	0.1565	0.0495	0.0839	1.4059	0.1828	0.0570	0.1042	1.5065	0.1934	0.0597	0.1165
0	100	SSDT [a]	1.1662	0.6619	0.2245	0.2746	1.7248	0.2075	0.0701	0.0871	2.1702	0.2791	0.0940	0.1183	2.6814	0.3628	0.1217	0.1557	3.0979	0.4168	0.1394	0.1815
		ZSDT[b]	1.1662	0.6618	0.2245	0.2744	1.7248	0.2075	0.0701	0.0870	2.1703	0.2791	0.0940	0.1182	2.6814	0.3628	0.1217	0.1557	3.0972	0.4168	0.1394	0.1814
		Present ct=0	1.1662	0.6618	0.2244	0.2749	1.7248	0.2075	0.0701	0.0871	2.1700	0.2791	0.0940	0.1183	2.6813	0.3628	0.1217	0.1558	3.0969	0.4166	0.1393	0.1816
		Present ct=0.01	1.1182	0.6335	0.2139	0.2674	1.6216	0.1946	0.0653	0.0837	2.0092	0.2575	0.0860	0.1126	2.4382	0.3284	0.1090	0.1465	2.7764	0.3716	0.1227	0.1692
		Present ct=0.02	1.0739	0.6073	0.2042	0.2604	1.5297	0.1830	0.0610	0.0806	1.8690	0.2387	0.0791	0.1074	2.2341	0.2996	0.0985	0.1385	2.5129	0.3346	0.1093	0.1588
		Present ct=0.1	0.8126	0.4531	0.1477	0.2177	1.0455	0.1225	0.0391	0.0633	1.1901	0.1480	0.0466	0.0810	1.3234	0.1716	0.0533	0.1001	1.4116	0.1808	0.0555	0.1115
100	100	SSDT [a]	1.1382	0.6453	0.2184	0.2702	1.6640	0.1999	0.0673	0.0850	2.0746	0.2663	0.0893	0.1148	2.5364	0.3423	0.1142	0.1502	2.9052	0.3897	0.1294	0.1741
		ZSDT[b]	1.1382	0.6452	0.2183	0.2700	1.6640	0.1999	0.0673	0.0850	2.0746	0.2663	0.0893	0.1148	2.5364	0.3423	0.1142	0.1501	2.9046	0.3897	0.1294	0.1740
		Present ct=0	1.1382	0.6453	0.2183	0.2705	1.6644	0.1999	0.0673	0.0851	2.0748	0.2663	0.0892	0.1149	2.5356	0.3422	0.1141	0.1502	2.9054	0.3897	0.1294	0.1742
		Present ct=0.01	1.0924	0.6182	0.2082	0.2633	1.5675	0.1878	0.0628	0.0818	1.9263	0.2464	0.0819	0.1095	2.3169	0.3113	0.1028	0.1418	2.6193	0.3495	0.1147	0.1631
		Present ct=0.02	1.0500	0.5932	0.1989	0.2566	1.4812	0.1770	0.0588	0.0789	1.7968	0.2290	0.0755	0.1047	2.1314	0.2851	0.0932	0.1344	2.3830	0.3164	0.1028	0.1536
		Present ct=0.1	0.7985	0.4448	0.1447	0.2154	1.0219	0.1195	0.0381	0.0624	1.1592	0.1438	0.0452	0.0797	1.2851	0.1662	0.0514	0.0984	1.3677	0.1747	0.0535	0.1094

[a]: Taken from Ref. Zenkour (2009); [b]: Taken from Ref. Thai and Choi (2014)

3. Results and discussion

In this section, the numerical results of the static and dynamic response of the simply supported P-FG plate resting visco-elastic foundation are presented to show the accuracy of the present theory. The properties of the materials used are

Ceramic (Al_2O_3): E_c=*380 GPa* and ρ_c=*3800 kg/m³*

Metal (Al): E_m=*70 GPa* and ρ_m=*2702 kg/m³*

For simplicity and because of the small effect of the Poisson's ratio on the FG-plate response (Akavci and Tanrikulu 2015). The Poisson's ratio is assumed to be constant through the P-FG plate thickness and equal to 0.3.

All results are computed in the dimensional formulations as

$$
\begin{aligned}
&w^* = \frac{100\ D_c}{q_0\ a^4} w\left(x=\frac{a}{2}, y=\frac{b}{2}\right),\\
&\overline{w} = \frac{10\ E_c h^3}{q_0\ a^4} w\left(x=\frac{a}{2}, y=\frac{b}{2}\right)\\
&\sigma_x^* = -\frac{h^2}{q_0\ a^2}\sigma_x\left(x=\frac{a}{2}, y=\frac{b}{2}, z=\frac{-h}{2}\right),\\
&\bar{\sigma}_x = -\frac{h^2}{q_0\ a^2}\sigma_x\left(x=\frac{a}{2}, y=\frac{b}{2}, z\right),\\
&\hat{\sigma}_x = -\frac{h}{q_0\ a}\sigma_x\left(x=\frac{a}{2}, y=\frac{b}{2}, z=\frac{h}{3}\right),\\
&\sigma_y^* = -\frac{h^2}{q_0\ a^2}\sigma_y\left(x=\frac{a}{2}, y=\frac{b}{2}, z=\frac{-h}{2}\right),\\
&\sigma_{xy}^* = \frac{h^2}{q_0\ a^2}\sigma_{xy}\left(x=0, y=0, z=\frac{-h}{2}\right),\\
&\bar{\sigma}_{xz} = \frac{h^2}{q_0\ a^2}\sigma_{xz}\left(x=0, y=\frac{b}{2}, z\right)
\end{aligned}
\tag{25}
$$

$$
\begin{aligned}
&\overline{\omega} = \omega h\sqrt{\frac{\rho_m}{E_m}},\quad \widehat{\omega} = \omega\frac{a^2}{h}\sqrt{\frac{\rho_m}{E_m}},\\
&D_m = \frac{E_m h^3}{12(1-\nu^2)},\ D_c = \frac{E_c h^3}{12(1-\nu^2)},\\
&ct = \frac{10^3 CT\ D_C}{a^4}\ k_0 = \frac{k_w a^4}{h^3},\\
&J_0 = \frac{k_{sx}a^2}{\nu h^3} = \frac{k_{sy}b^2}{\nu h^3},\\
&\bar{k}_w = \frac{k_w a^4}{D_m},\ k\_s = (k\_s\ \ a\text{^}2)/D\_m
\end{aligned}
$$

3.1 bending analysis of P-FG plate

In this first part, the obtained results are for bending analysis of the simply supported P-FG plate.

Table 1 presents the non-dimensional displacement (w^*) and stresses (σ_x^*, σ_y^* and σ_{xy}^*) of the P-FG plate under uniform transverse mechanical load $q(x,y)$ for various material index (p) and foundation parameters (K_0, J_0 and ct). The obtained results are compared with those given by Zenkour (2009) employing SSDT and Thai and Choi (2014) using zeroth-order shear deformation theory. A good agreement are confirmed between the current results and those published by Zenkour (2009) and Thai and Choi (2014). It is clear from the results that the increases in the damping coefficient (ct) and foundation parameter (K_0, J_0) lead to decrease the non-dimensional displacement (w^*) and stresses (σ_x^*, σ_y^* and σ_{xy}^*). It can

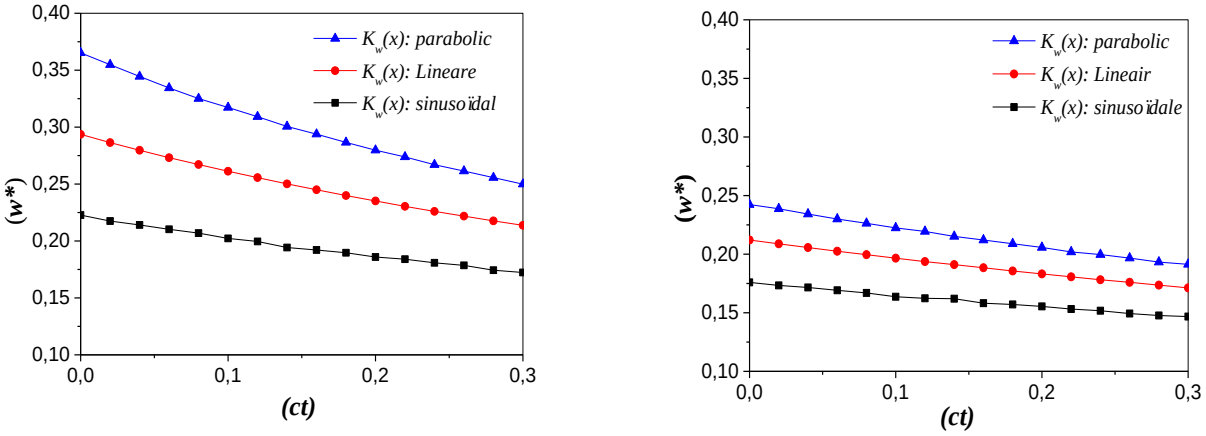

(a) rectangular FG-plate (b) square FG-plate

Fig. 2 Effect of foundation parameters $(K_w(x), ct)$ on dimensionless deflection (w^*) of (a):square plate $(a=b)$, and (b): rectangular pate $(b=3a)$ reposed on viscoelastic foundation under sinusoidal loads with $(a/h=5, p=2, \zeta=20 \text{ and } k_w=k_s=100)$

Table 2 Dimensionless deflection $(\bar{w})$ and stress $(\bar{\sigma}_x)$ of square plates under sinusoidal loads (k_W=k_s=0)

Method	P=1						P=4						P=10					
	$\bar{\sigma}_x(h/3)$			$\bar{w}$			$\bar{\sigma}_x(h/3)$			$\bar{w}$			$\bar{\sigma}_x(h/3)$			$\bar{w}$		
	a/h=4	a/h=10	a/h=100	a/h=4	a/h=10	a/h=100	a/h=4	a/h=10	a/h=100	a/h=4	a/h=10	a/h=100	a/h=4	a/h=10	a/h=100	a/h=4	a/h=10	a/h=100
Quasi-3D[a]	0.5925	1.4945	14.9690	0.6997	0.5845	0.5624	0.4404	1.1783	11.9320	1.1178	0.8750	0.8286	0.3227	1.1783	11.9320	1.3490	0.8750	0.8286
Quasi-3D [b]	0.5910	1.4917	14.9440	0.7020	0.5868	0.5648	0.4340	1.1593	11.7380	1.1095	0.8698	0.8241	0.3108	0.8467	8.6013	1.3327	0.9886	0.9228
Quasi-3D[c]	0.5911	1.4917	14.9450	0.7020	0.5868	0.5647	0.4330	1.1588	11.7370	1.1108	0.8700	0.8240	0.3097	0.8462	8.6010	1.3334	0.9888	0.9227
Quasi-3D[d]	0.6221	1.5064	14.9690	0.7171	0.5875	0.5625	0.4877	1.1971	11.9230	1.1585	0.8821	0.8286	0.3695	0.8965	8.6077	1.3745	1.0072	0.9361
Quasi-3D[e]	0.6221	1.5064	14.9690	0.7171	0.5875	0.5625	0.4877	1.1971	11.9230	1.1585	0.8821	0.8286	0.3695	0.8965	8.6077	1.3745	1.0072	0.9361
FSDT [d]	0.8060	2.0150	20.1500	0.7291	0.5889	0.5625	0.6420	1.6049	16.0490	1.1125	0.8736	0.8286	0.4796	1.1990	11.9900	1.3178	0.9966	0.9360
CPT[d]	0.8060	2.0150	20.1500	0.5623	0.5623	0.5623	0.6420	1.6049	16.0490	0.8281	0.8281	0.8281	0.4796	1.1990	11.9900	0.9354	0.9354	0.9354
ZSDT[f]	0.5812	1.4898	14.9676	0.7284	0.5890	0.5625	0.4449	1.1794	11.9209	1.1599	0.8815	0.8287	0.3259	0.8785	8.9060	1.3909	1.0087	0.9362
Present ct=0	0.5803	1.4894	14.9675	0.7280	0.5889	0.5625	0.4424	1.1783	11.9208	1.1619	0.8819	0.8287	0.3235	0.8775	8.9059	1.3917	1.0089	0.9362
Present ct=0.01	0.5616	1.4501	14.5936	0.7046	0.5734	0.5485	0.4201	1.1324	11.4842	1.1035	0.8475	0.7983	0.3041	0.8388	8.5403	1.3084	0.9644	0.8978
Present ct=0.02	0.5440	1.4129	14.2303	0.6825	0.5587	0.5348	0.3998	1.0902	11.0763	1.0502	0.8159	0.7700	0.2869	0.8034	8.2017	1.2343	0.9237	0.8622
Present ct=0.1	0.4353	1.1729	11.9047	0.5461	0.4638	0.4474	0.2887	0.8394	8.6412	0.7584	0.6282	0.6007	0.1976	0.6002	6.2339	0.8499	0.6901	0.6553

[a]: Taken from Ref. Neves *et al*. (2012b); [b]: Taken from Ref. Neves *et al.* (2012a); [c]: Taken from Ref. Neves *et al*. (2013); [d]: Taken from Ref . Carrera *et al*. 2008; [e]: Taken from Ref. Carrera *et al.* 2011; [f]: Taken from Ref. Thai and Choi (2014)

be seen also that the deflection (w*) is in direct correlation relation with material index (p).

Table 2 shows dimensionless deflection $(\bar{w})$ and stress $(\bar{\sigma}_x)$ of square thin and thick plates under sinusoidal load versus material index (p=1,4 and 10) and geometry ratio $(4 \le a/h \le 100)$. The current results are compared with those computed via quasi-3D solutions of (Carrera *et al.* 2008, 2011, Neves *et al*. 2012a, b, 2013), ZSDT of Thai and Choi (2014), and CPT and FSDT given by Carrera *et al.* (2008). It is clear from the table that the obtained results are in good agreement with ZSDT and quasi-3D solutions. The CPT model underestimates the dimensionless deflection $(\bar{w})$ because of the omission of the transverse shear deformation effect. It can be seen also that the FSDT give only the good results of displacement $(\bar{w})$ and almost the same values of the stress $(\bar{\sigma}_x)$ with those computed via CPT model.

From the current result it can be also observed that the deflection $(\bar{w})$ and axial stress $(\bar{\sigma}_x)$ are in inverse relation with the damping coefficient (ct). The lower values of transversal displacement $(\bar{w})$ are obtained for thin plate.

Fig. 2 plots the variation of the dimensionless deflection (w^*) of square and rectangular P-FG plate (p=2) under sinusoidal loads and reposed on viscoelastic foundation with $(a/h=5, k_w=k_s=100)$. The dimensionless deflection (w^*) is plotted versus the Damping parameter (ct) for linear, parabolic and sinusoidal variation of the Winkler parameters. From the presented graphs, it can be seen that the dimensionless deflection (w^*) s in inverse relation with damping coefficient (ct), whatever the type of

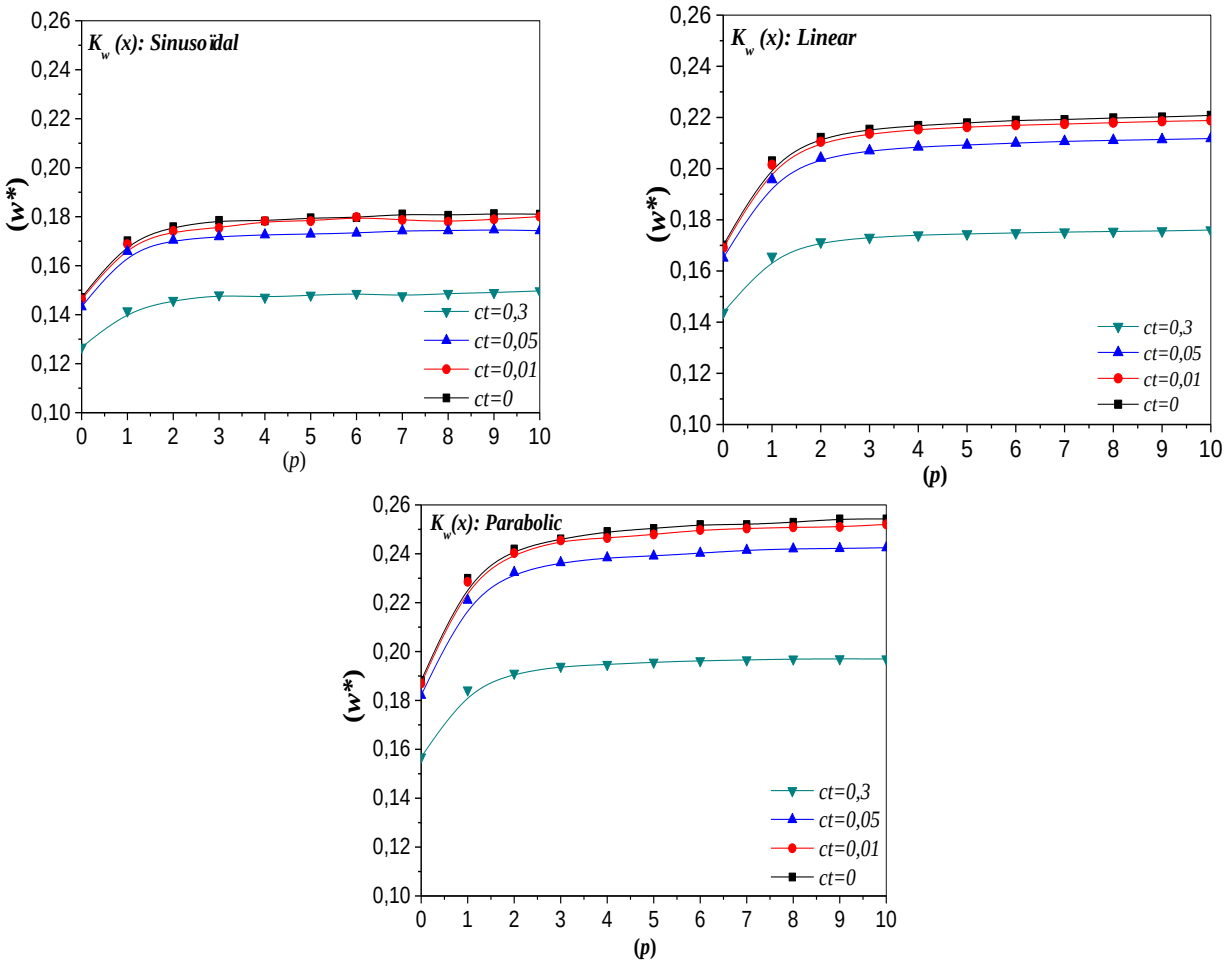

Fig. 3 Effect of foundation parameters $(K_w(x), ct)$ and power law index (p) on dimensionless deflection (w^*) of square plate $(a=b)$ reposed on visco-elastic foundation under sinusoidal loads with $(a/h=5,\ \zeta=20\ and\ k_w=k_s=100)$

the FG-plate (square or rectangular). It is clear from the results that the lower values of dimensionless deflection (w^*) are obtained for plate with sinusoidal variation of the elastic foundation parameter $K_w(x)$ (Winkler). It can be noted that the increase in the aspect ratio (b/a) leads to increase the dimensionless deflection (w^*) because the plate become flexible.

Effect of foundation parameters $(K_w(x), ct)$, power law index (p) on dimensionless deflection (w^*) of square thick FG-plate $(a=b)$ resting on visco-elastic foundation under sinusoidal load (q) is illustrated in Fig. 3. The plate has geometry ratio $(a/h=5)$ and parameters $(\zeta=20, k_w=k_s=100)$. From the obtained curves, it can be noted that the increase of the damping parameter (ct) leads to decrease the values of (w^*). We can observe from the graphs that the smaller values of (w^*) are obtained for sinusoidal variation of Winkler parameter $(K_w(x))$ and the biggest values are obtained for parabolic variation and the results of (w^*) of plate on elastic foundation with linear variation of winkler parameter are between the values of the two types mentioned before. We can confirm once again that the dimensionless deflection (w^*) is in direct correlation relation with power index (p).

Fig. 4 shows the variation of dimensionless deflection (w^*) of thick FG-plate on visco-elastic foundation under sinusoidal load versus the damping coefficient (ct) and parameter (ζ) for various type of the elastic foundation variation: sinusoidal, linear and parabolic with $(a/h=5, p=2, a=b\ and\ k_w=k_s=100)$. We can see from the results that the increase of the values of the damping coefficients (ct) and the parameters (ζ) lead to decrease the values of the non-dimensional deflection (w^*) of square simply supported FG-plate.

Fig. 5 illustrates the variations of dimensionless in-plane normal stresses $(\overline{\sigma_x})$ through the thickness (z/h) of square FG-plates reposed on viscoelastic foundation $(\zeta=20\ and\ k_w=k_s=100)$ versus the damping coefficient (ct). The graphs are plotted for various type of $K_w(x)$ (sinusoidal, linear and parabolic) with thickness ratio $(a/h=5)$ and power index $(p=2)$. The obtained curves show

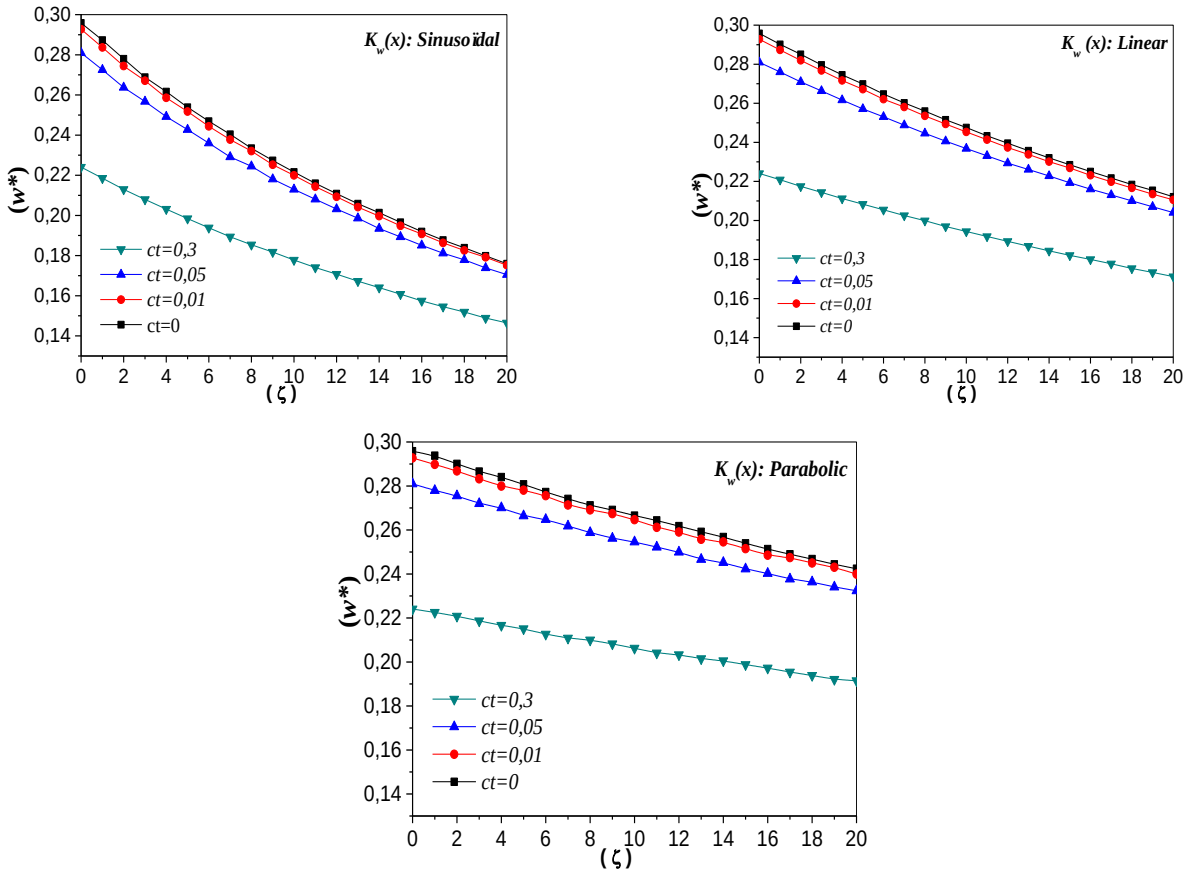

Fig. 4 Effect of foundation parameters $(K_w(x),\ ct\ and\ \zeta)$ on dimensionless deflection (w^*) of square plate $(a=b)$ reposed on visco-elastic foundation under sinusoidal loads with $(a/h=5,\ p=2\ and\ k_w=k_s=100)$

that the increase in the damping coefficient (ct) leads to a reduction of the normal axial stress $(\overline{\sigma_x})$ at the upper and lower surfaces of the FG- plate. We can see that the biggest values of the stress $(\overline{\sigma_x})$ are obtained when the FG-plate is resting on the elastic foundation with parabolic variation of the Winkler parameter $K_w(x)$.

Fig. 6 presents Influence of the foundation parameters $(K_w(x), ct)$ on dimensionless stress $(\overline{\sigma_x})$ of square plate $(a=b)$ and rectangular plate $(b=3a)$ resting on sinusoidal, linear and parabolic visco-elastic foundation with $(a/h=5,\ p=2\ and\ k_w=k_s=100)$. We observe from the results that the increase of the damping parameter (ct) leads to a reduction the values of the axial stress $(\overline{\sigma_x})$, whatever the type of variation of the Winkler parameter $(K_w(x))$.

We can conclude that the damping parameter (ct), aspect ratio (b/a) and variation of the elastic foundation have a significant role on dimensionless axial stress $(\overline{\sigma_x})$.

The variations of dimensionless transverse shear stress $(\overline{\sigma_{xz}})$ through the thickness (z/h) of square FG-plates FGM on various visco-elastic foundations in function of damping coefficients (ct) are illustrated in Fig. 7. The plate has $a/h=5$, $p=2$ and $k_w=k_s=100$. From the graphs, we can see that the maximum transverse shear stress $(\overline{\sigma_{xz}})$ is obtained for plate on parabolic visco-elastic foundation. It can be also observed that the increase in the value of (ct) leads to decrease the values of $(\overline{\sigma_{xz}})$.

The current results are compared with those given by Baferani *et al.* (2011) using TSDT model and those computed via ZSDT by Thai and Choi (2014). From the performed comparisons, a good agreement is confirmed between the present result and those found in the literature (Baferani *et al.* 2011, Thai and Choi 2014). It is also observed from the results that the dimensionless fundamental frequency $(\hat{\omega})$ increase with the increase of the damping coefficient (ct), Winkler and Pasternak parameters (k_w, k_s). It is clear that the (k_s) parameter (effect of Pasternak shear layer) has dominant influence on increasing the non-dimensional fundamental frequency $(\hat{\omega})$.

It can be also noted that the increase on the values of the power index (p) leads to decrease the dimensionless frequency $(\hat{\omega})$ because the plate become supple.

The values of the dimensionless fundamental frequency $(\overline{\omega})$ of simply supported P-FG plate resting on visco-elasticfoundation with $(k_w=k_s=100)$ are presented in the Table 4.

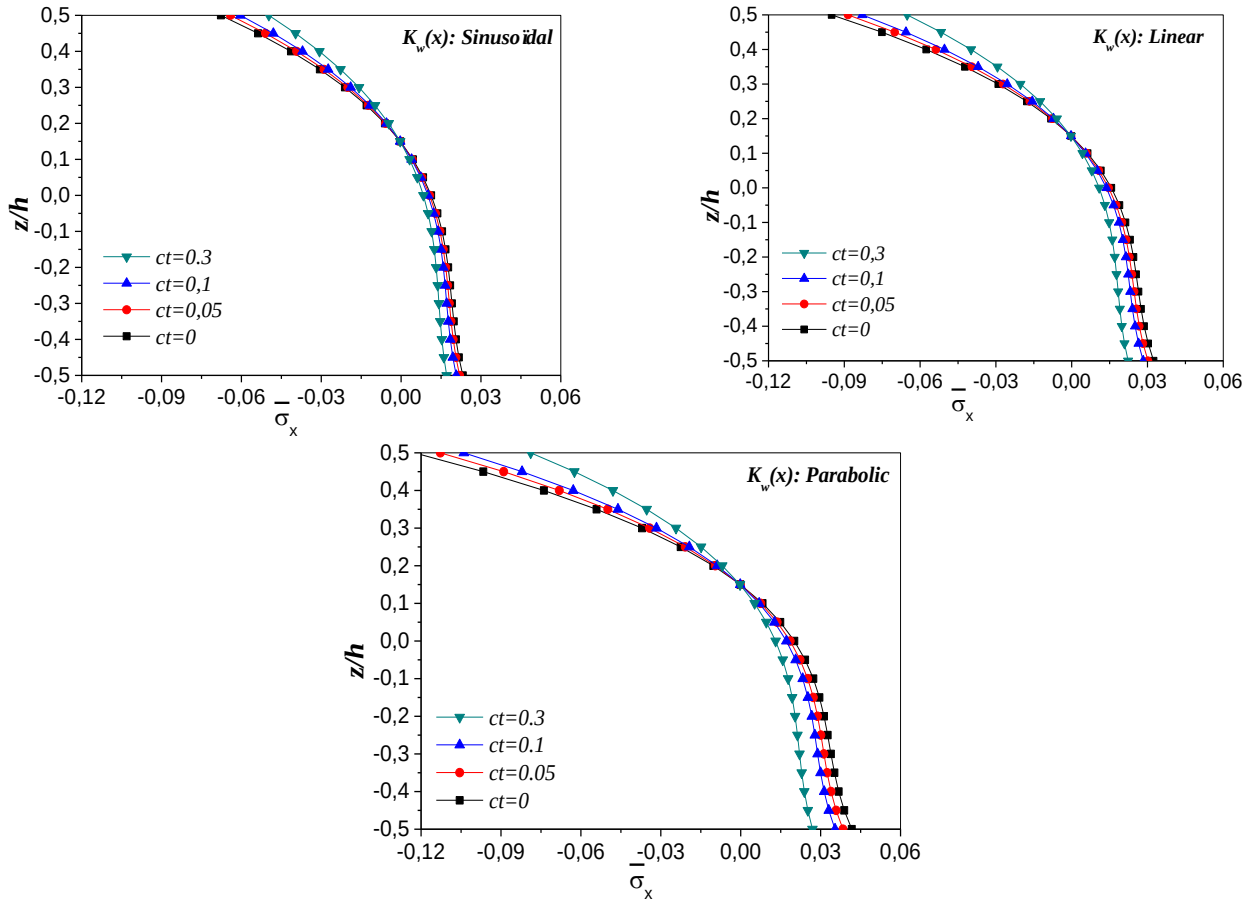

Fig. 5 Variations of dimensionless stresses $(\overline{\sigma_x})$ through the thickness (z/h) of square FG-plate reposed on visco-elastic foundation with deferent type of parameters $(K_w(x), ct)$ under sinusoidal load $(a/h=5,\ p=2, \zeta=20\ and\ k_w=k_s=100)$

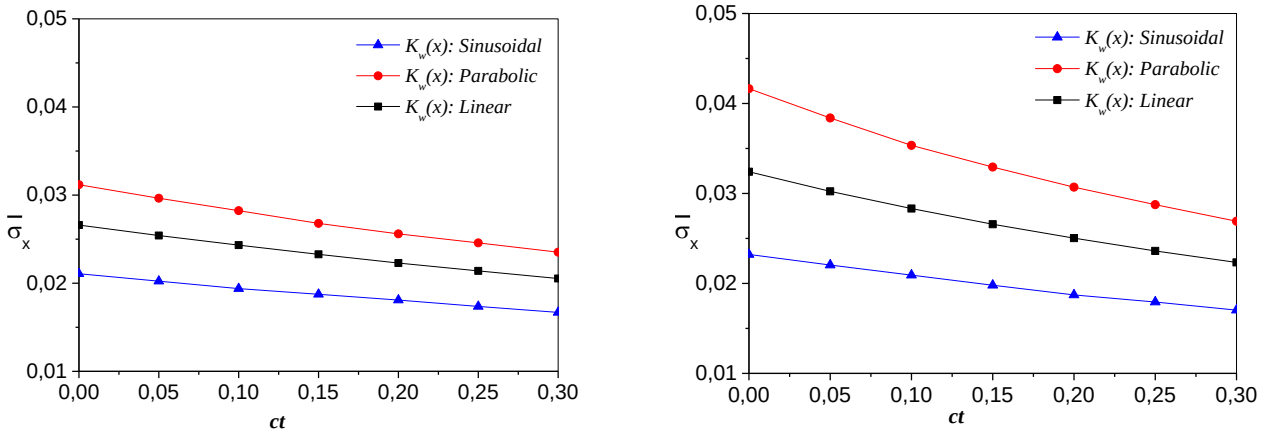

(a) rectangular FG-plate (b) square FG-plate

Fig. 6 Effect of foundation parameters $(K_w(x), ct)$ on dimensionless stresses $(\overline{\sigma_x}(a/2, b/2, h/2))$ of (a): square plate $(a=b)$, and (b): rectangular pate $(b=3a)$ reposed on visco-elastic foundation under sinusoidal loads with $(a/h=5,\ p=2, \zeta=20\ and\ k_w=k_s=100)$

The computed results are compared with those generated by Thai and Choi (2012) and (2014) based on RPT model and ZSDT models, respectively.

The effects of the aspect ratio (b/a), damping coefficient (ct), and elastic foundation variation type (sinusoidal, linear and parabolic) on dimensionless

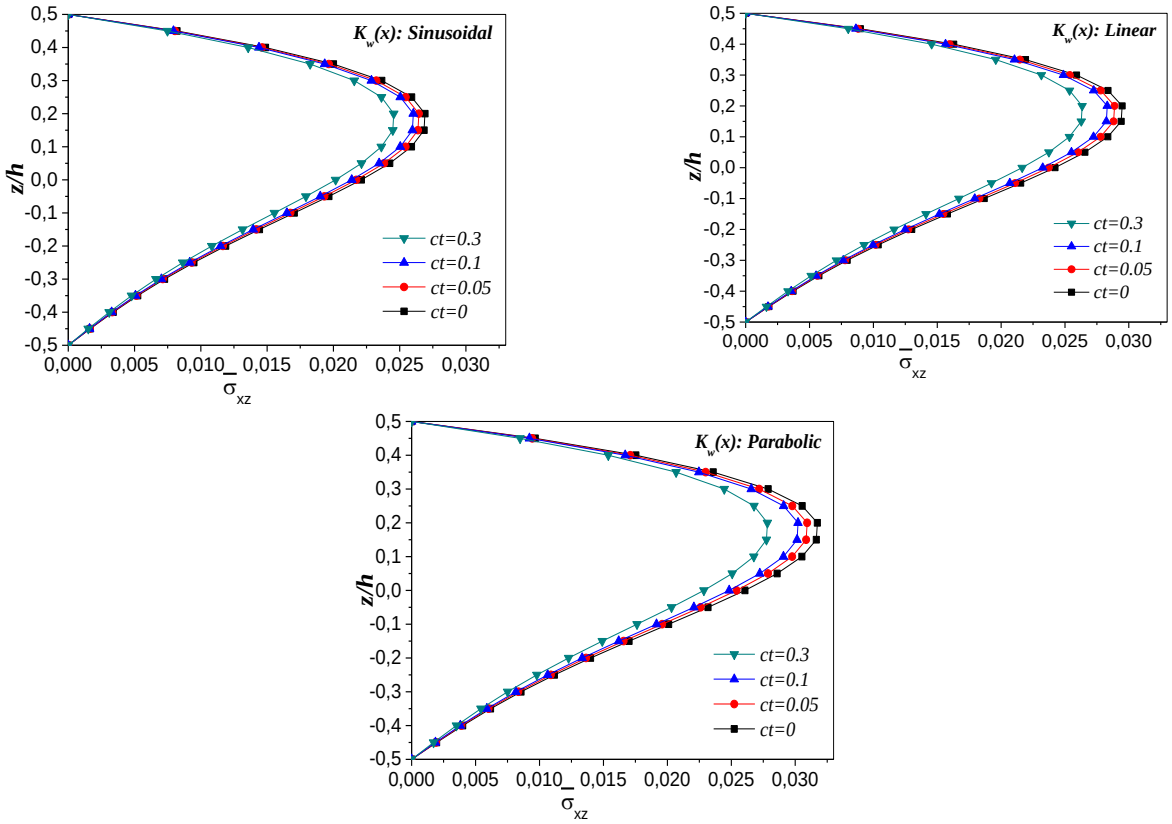

Fig. 7 Variations of dimensionless stresses $(\overline{\sigma_{xz}})$ through the thickness (z/h) of square FG-plates reposed on visco-elastic foundation with deferent type of parameters $(K_w(x), ct)$ under sinusoidal loads $(a/h=5,\ p=2, \zeta=20\ and\ k_w=k_s=100)$

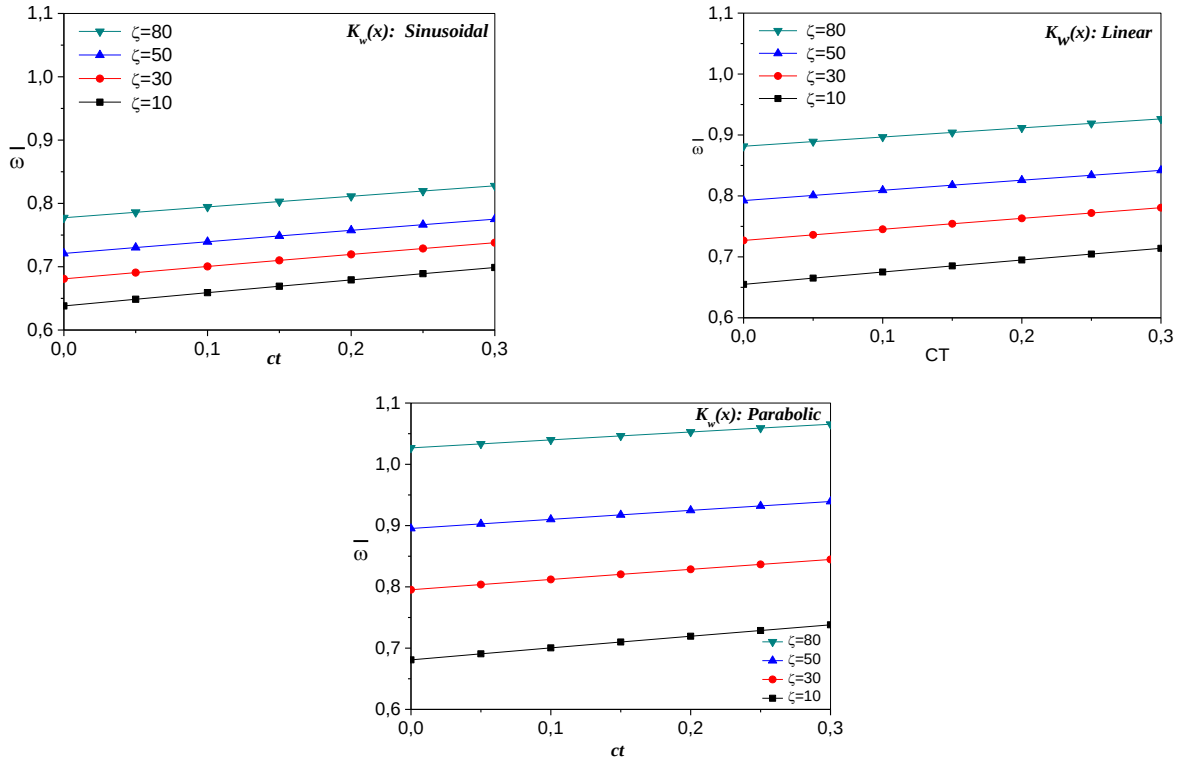

Fig. 8 Effect of foundation parameters $(K_w(x), ct\, and\, \zeta)$ on dimensionless fundamental frequency $(\overline{\omega})$ of square plates $(a/h=5,\ p=2\, and\ k_w=k_s=100)$

Table 3 Dimensionless fundamental frequency $\hat{\omega}$ of square plates

h/a	Method	$(k_w,k_s)=(0,0)$					$(k_w,k_s)=(0,100)$					$(k_w,k_s)=(100,0)$					$(k_w,k_s)=(100,100)$				
		p=0	p=0.5	p=1	p=2	p=5	p=0	p=0.5	p=1	p=2	p=5	p=0	p=0.5	p=1	p=2	p=5	p=0	p=0.5	p=1	p=2	p=5
0.05	TSDT [a]	0.0291	0.0249	0.0227	0.0209	0.0197	0.0406	0.0389	0.0382	0.0380	0.0381	0.0298	0.0258	0.0238	0.0221	0.0210	0.041	0.04	0.039	0.039	0.039
	ZSDT[b]	0.0291	0.0246	0.0222	0.0202	0.0191	0.0406	0.0386	0.0378	0.0374	0.0377	0.0298	0.0255	0.0233	0.0214	0.0204	0.0411	0.0392	0.0384	0.0381	0.0384
	Present ct=0	0.0291	0.0246	0.0222	0.0202	0.0191	0.0406	0.0386	0.0378	0.0374	0.0377	0.0298	0.0255	0.0233	0.0214	0.0204	0.0411	0.0392	0.0384	0.0381	0.0384
	Present ct=0.01	0.0293	0.0249	0.0225	0.0205	0.0195	0.0407	0.0388	0.0380	0.0376	0.0378	0.0332	0.0298	0.0281	0.0269	0.0264	0.0436	0.0421	0.0415	0.0414	0.0419
	Present ct=0.02	0.0295	0.0251	0.0228	0.0209	0.0198	0.0408	0.0390	0.0381	0.0377	0.0380	0.0333	0.0300	0.0283	0.0271	0.0267	0.0437	0.0423	0.0417	0.0415	0.0420
	Present ct=0.1	0.0309	0.0270	0.0249	0.0233	0.0226	0.0419	0.0402	0.0395	0.0392	0.0395	0.0346	0.0316	0.0301	0.0291	0.029	0.0447	0.0434	0.0429	0.0428	0.0434
0.1	TSDT [a]	0.1134	0.0975	0.0891	0.0819	0.0767	0.1599	0.1540	0.1517	0.1508	0.1515	0.116	0.101	0.093	0.087	0.082	0.1619	0.1563	0.1542	0.1535	0.1543
	ZSDT[b]	0.1134	0.0963	0.0868	0.0788	0.0740	0.1597	0.1526	0.1494	0.1478	0.1487	0.1161	0.0999	0.0910	0.0836	0.0795	0.1617	0.1549	0.1519	0.1505	0.1515
	Present ct=0	0.1134	0.0963	0.0868	0.0788	0.0740	0.1597	0.1526	0.1494	0.1478	0.1487	0.1161	0.0999	0.0910	0.0836	0.0795	0.1617	0.1549	0.1519	0.1505	0.1515
	Present ct=0.01	0.1141	0.0973	0.0880	0.0801	0.0755	0.1603	0.1532	0.1501	0.1485	0.1495	0.1299	0.1172	0.1106	0.1057	0.1037	0.1719	0.1665	0.1644	0.1637	0.1655
	Present ct=0.02	0.1149	0.0983	0.0891	0.0814	0.0770	0.1608	0.1538	0.1508	0.1492	0.1502	0.1306	0.1180	0.1115	0.1067	0.1048	0.1724	0.1671	0.1650	0.1644	0.1662
	Present ct=0.1	0.1208	0.1058	0.0978	0.0914	0.0881	0.1651	0.1588	0.1561	0.1549	0.1562	0.1358	0.1243	0.1186	0.1145	0.1132	0.1764	0.1717	0.1698	0.1696	0.1716
0.15	TSDT [a]	0.2454	0.2121	0.1939	0.1778	0.1648	0.3515	0.3407	0.3365	0.3351	0.3362	0.2519	0.2204	0.2036	0.1889	0.1775	0.356	0.346	0.342	0.341	0.343
	ZSDT[b]	0.2452	0.2090	0.1885	0.1706	0.1589	0.3512	0.3369	0.3304	0.3269	0.3286	0.2516	0.2173	0.1982	0.1818	0.1716	0.3557	0.3421	0.3359	0.3329	0.3349
	Present ct=0	0.2452	0.2090	0.1885	0.1706	0.1588	0.3512	0.3369	0.3304	0.3269	0.3286	0.2516	0.2173	0.1982	0.1818	0.1715	0.3557	0.3421	0.3359	0.3329	0.3349
	Present ct=0.01	0.2470	0.2113	0.1912	0.1737	0.1624	0.3524	0.3384	0.3319	0.3285	0.3303	0.2832	0.2567	0.2428	0.2320	0.2270	0.3787	0.3684	0.3640	0.3627	0.3663
	Present ct=0.02	0.2487	0.2136	0.1938	0.1768	0.1658	0.3537	0.3398	0.3334	0.3301	0.3320	0.2848	0.2585	0.2448	0.2343	0.2295	0.3799	0.3697	0.3654	0.3641	0.3678
	Present ct=0.1	0.2624	0.2308	0.2137	0.1995	0.1914	0.3634	0.3509	0.3453	0.3428	0.3454	0.2967	0.2730	0.2609	0.2519	0.2485	0.3889	0.3799	0.3763	0.3757	0.3800
0.2	TSDT [a]	0.4154	0.3606	0.3299	0.3016	0.2765	0.6080	0.5932	0.5876	0.5861	0.5879	0.427	0.376	0.348	0.322	0.3	0.616	0.603	0.598	0.597	0.599
	ZSDT[b]	0.4151	0.3551	0.3205	0.2892	0.2667	0.6075	0.5858	0.5753	0.5694	0.5722	0.4269	0.3702	0.3381	0.3097	0.2901	0.6156	0.5950	0.5852	0.5800	0.5843
	Present ct=0	0.4151	0.3551	0.3205	0.2892	0.2665	0.6075	0.5858	0.5753	0.5694	0.5722	0.4269	0.3702	0.3381	0.3096	0.2900	0.6156	0.5950	0.5852	0.5800	0.5833
	Present ct=0.01	0.4184	0.3593	0.3254	0.2949	0.2731	0.6097	0.5883	0.5780	0.5723	0.5752	0.4846	0.4417	0.4187	0.4003	0.3908	0.6569	0.6418	0.6351	0.6327	0.6389
	Present ct=0.02	0.4216	0.3634	0.3302	0.3005	0.2795	0.6119	0.5908	0.5807	0.5752	0.5783	0.4874	0.4451	0.4225	0.4045	0.3953	0.6590	0.6442	0.6375	0.6353	0.6416
	Present ct=0.1	0.4465	0.3949	0.3663	0.3418	0.3262	0.6294	0.6107	0.6019	0.5977	0.6020	0.5091	0.4711	0.4512	0.4360	0.4296	0.6752	0.6624	0.6569	0.6557	0.6629

[a]: Taken from Ref. Baferani *et al.* (2011); [b]: Taken from Ref. Thai and Choi (2014)

Table 4 Dimensionless fundamental frequency $\bar{\omega}$ of square plates $\left(\bar{k}_w=\bar{k}_s=100\right)$

a/	Method	a/b = 0.5						a/b = 1						a/b = 2					
		P=0	P=0.5	P=1	P=2	P=5	P=10	P=0	P=0.5	P=1	P=2	P=5	P=10	P=0	P=0.5	P=1	P=2	P=5	P=10
5	RPT[a]	11.3952	11.2331	11.1780	11.2018	11.3593	11.3298	15.3904	14.8757	14.6305	14.3860	12.4291	11.3298	28.6467	26.8009	25.7640	24.9077	24.5036	24.4352
	ZSDT[b]	11.3952	11.2331	11.1780	11.2018	11.3593	11.4558	15.3904	14.8757	14.6305	14.5004	14.5843	14.6636	28.6467	26.8009	25.7640	24.9077	24.5036	24.4352
	Present ct=0	11.3955	11.2333	11.1781	11.2018	11.3588	11.4557	15.3914	14.8762	14.6309	14.5004	14.5833	14.6634	28.6537	26.8051	25.7675	24.9092	24.4991	24.4352
	Present ct=0.01	11.4704	11.3172	11.2668	11.2951	11.4565	11.5557	15.4462	14.9388	14.6977	14.5713	14.6581	14.7404	28.6824	26.8387	25.8040	24.9486	24.5419	24.4800
	Present ct=0.02	11.5448	11.4004	11.3548	11.3876	11.5533	11.6549	15.5008	15.0010	14.7641	14.6418	14.7326	14.8171	28.7110	26.8722	25.8403	24.9880	24.5846	24.5246
	Present ct=0.1	12.1234	12.0454	12.0353	12.1020	12.2997	12.4190	15.9310	15.4898	15.2852	15.1939	15.3146	15.4160	28.9389	27.1384	26.1292	25.3001	24.9234	24.8787
10	RPT[a]	11.7257	11.4992	11.4270	11.4530	11.6243	11.7093	16.1728	15.4895	15.1887	15.0455	15.1497	15.2045	32.3893	29.7133	28.3322	27.2931	24.8582	22.6596
	ZSDT[b]	11.7257	11.4992	11.4270	11.4530	11.6243	11.7093	16.1728	15.4895	15.1887	15.0455	15.1497	15.2045	32.3893	29.7133	28.3322	27.2931	26.8741	26.6964
	Present ct=0	11.7258	11.4992	11.4270	11.4529	11.6240	11.7092	16.1731	15.4896	15.1888	15.0454	15.1489	15.2043	32.3915	29.7149	28.3334	27.2928	26.8689	26.6947
	Present ct=0.01	11.8002	11.5832	11.5162	11.5470	11.7225	11.8100	16.2269	15.5517	15.2556	15.1167	15.2242	15.2816	32.4180	29.7467	28.3686	27.3313	26.9105	26.7380
	Present ct=0.02	11.8742	11.6665	11.6046	11.6403	11.8202	11.9099	16.2805	15.6135	15.3221	15.1877	15.2991	15.3585	32.4444	29.7785	28.4037	27.3698	26.9521	26.7813
	Present ct=0.1	12.4499	12.3126	12.2890	12.3616	12.5746	12.6811	16.7029	16.0995	15.8438	15.7439	15.8855	15.9605	32.6548	30.0315	28.6830	27.6758	27.2826	27.1249
20	RPT[a]	11.8246	11.5780	11.5005	11.5273	11.7054	11.7886	16.4249	15.6851	15.3663	15.2209	15.3414	15.3929	33.8869	30.8606	29.3467	28.2628	27.9294	27.7426
	ZSDT[b]	11.8246	11.5780	11.5005	11.5273	11.7054	11.7886	16.4249	15.6851	15.3663	15.2209	15.3414	15.3929	33.8869	30.8606	29.3467	28.2628	27.9294	27.7426
	Present ct=0	11.8246	11.5780	11.5005	11.5273	11.7053	11.7885	16.4249	15.6851	15.3663	15.2209	15.3412	15.3928	33.8875	30.8610	29.3470	28.2626	27.9273	27.7418
	Present ct=0.01	11.8989	11.6620	11.5897	11.6215	11.8040	11.8895	16.4785	15.7471	15.4331	15.2923	15.4165	15.4702	33.9134	30.8924	29.3819	28.3009	27.9685	27.7845
	Present ct=0.02	11.9728	11.7453	11.6782	11.7151	11.9019	11.9896	16.5318	15.8089	15.4996	15.3633	15.4914	15.5471	33.9392	30.9238	29.4166	28.3391	28.0096	27.8271
	Present ct=0.1	12.5479	12.3919	12.3638	12.4380	12.6578	12.7620	16.9524	16.2942	16.0217	15.9205	16.0784	16.1493	34.1449	31.1733	29.6933	28.6429	28.3363	28.1659

[a]: Taken from Ref. Thai and Choi (2012); [b]: Taken from Ref. Thai and Choi (2014)

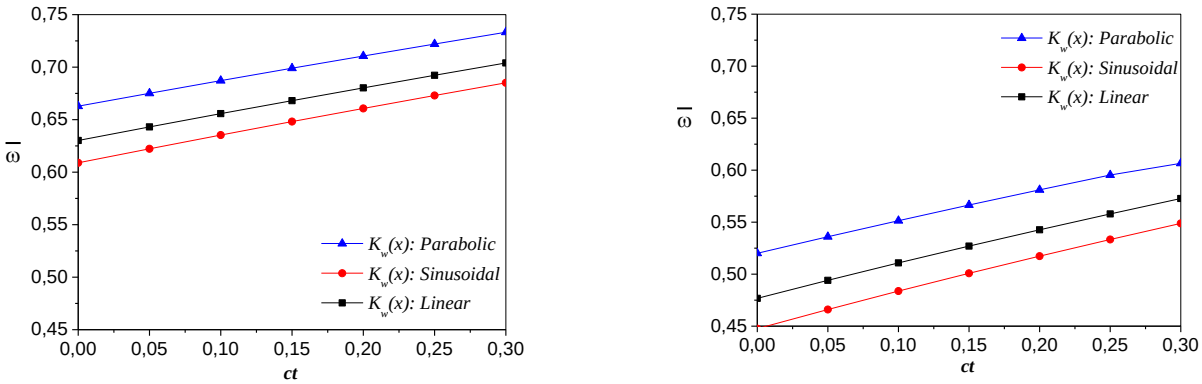

square FG-plate $(b=a)$ rectangular FG-plate $(b=3a)$

Fig. 9 Effect of foundation parameters $(K_w(x), ct)$ and (b/a) on dimensionless fundamental frequency $(\bar{\omega})$ of FG-plates $(a/h=5,\ p=2, \zeta=20 \text{ and } k_w=k_s=100)$

fundamental frequency $(\bar{\omega})$ of thick FG-plate with $(a/h=5,\ p=2, \zeta=20 \text{ and } k_w=k_s=100)$ are illustrated in Fig. 9. It can be confirmed that the increase in the values of the damping parameter (ct) leads to increase the fundamental frequency $(\bar{\omega})$ but this last decrease with the increase of the aspect ratio (b/a). The effect of the variation of the elastic foundation has an important role on the values of the fundamental frequency $(\bar{\omega})$

4. Conclusions

In the present paper, a simple shear deformation integral plate model is derived for the bending and free vibration analyses of FG plates resting on variable visco-Pasternak foundations. The Winkler parameter is varying in the direction of x-axis as linear, parabolic and sinusoidal functions of x. The present theory take into account the transverse shear deformation effect without using the shear correction factors. The volume fractions of the constituents and, hence, the effective material properties of FG-plate are assumed to vary in the thickness direction only according to power law model. The equations of motion are determined and resolved via Hamilton's principle and Navier solutions, respectively. The comparison of the obtained numerical results with those found in the literature show that the current theory gives a very good prediction of deflection, stress and fundamental frequency of FG plates resting on elastic foundation. The results also indicate that the inclusion of visco-Pasternak foundation parameters will increase the stiffness of the FG-plate, and hence, leads to a reduction of central deflection and an increase in fundamental frequency. Other works can be carried out in future by considering other types of materials (Panjehpour *et al.* 2018, Othman and Fekry 2018, Ahmed *et al*. 2020, Abed and Majeed 2020, Akbaş 2020a, b, Mercan *et al*. 2020, Fenjan *et al.* 2020b, c, Liu *et al*. 2020, Timesli 2020, Patnaik *et al.* 2020, Yuan *et al.* 2020, Mansour and Fayed 2021, Rashidpour *et al*. 2021, Shakouri 2021).

References

Abdelrahman, W.G. (2020), "Effect of material transverse distribution profile on buckling of thick functionally graded material plates according to TSDT", *Struct. Eng. Mech.*, **74**(1), 83-90. https://doi.org/10.12989/sem.2020.74.1.08.

Abdulrazzaq, M.A. Fenjan, R.M Ahmed, R.A. and Faleh, N.M. (2020), "Thermal buckling of nonlocal clamped exponentially graded plate according to a secant function based refined theory", *Steel Compos. Struct.*, **35**(1), 147-157. http://doi.org/10.12989/scs.2020.35.1.147.

Abed, Z.A.K. and Majeed, W.I. (2020), "Effect of boundary conditions on harmonic response of laminated plates", *Compos. Mater. Eng.*, **2**(2). 125-140. https://doi.org/10.12989/cme.2020.2.2.125.

Ahmed, R.A., Fenjan, R.M. and Faleh, N.M. (2019), "Analyzing post-buckling behavior of continuously graded FG nanobeams with geometrical imperfections", *Geomech. Eng.*, **17**(2), 175-180. https://doi.org/10.12989/gae.2019.17.2.175.

Ahmed, R.A., Moustafa, N.M., Faleh, N.M. and Fenjan, R.M. (2020), "Nonlocal nonlinear stability of higher-order porous beams via Chebyshev-Ritz method", *Struct. Eng. Mech.*, **76**(3), 413-420. http://doi.org/10.12989/sem.2020.76.3.413.

Akavci, S.S. and Tanrikulu, A.H. (2015), "Static and free vibration analysis of functionally graded plates based on a new quasi-3D and 2D shear deformation theories", *Compos. Part B*, **83**, 203-215. https://doi.org/10.1016/j.compositesb.2015.08.043.

Akbaş, Ş.D. (2020a), "Dynamic responses of laminated beams under a moving load in thermal environment", *Steel Compos. Struct.*, **35**(6), 729-737. https://doi.org/10.12989/scs.2020.35.6.729.

Akbaş, Ş.D. (2015), "Wave propagation of a functionally graded beam in thermal environments", *Steel Compos. Struct.*, **19**(6), 1421-1447. https://doi.org/10.12989/scs.2015.19.6.1421.

Akbaş, Ş.D. (2020b), "Modal analysis of viscoelastic nanorods under an axially harmonic load", *Adv. Nano Res.*, **8**(4), 277-282. http://doi.org/10.12989/anr.2020.8.4.277.

Akgün, G. and Kurtaran, H. (2019), "Large displacement transient analysis of FGM super-elliptic shells using GDQ method", *Thin-Wall. Struct.*, **141**, 133-152. https://doi.org/10.1016/j.tws.2019.03.049.

Al-Basyouni, K.S., Ghandourah, E., Mostafa, H.M. and Algarni, A. (2020), "Effect of the rotation on the thermal stress wave propagation in non-homogeneous viscoelastic body", *Geomech. Eng.*, **21**(1), 1-9. https://doi.org/10.12989/gae.2020.21.1.001.

Avcar, M. (2019), "Free vibration of imperfect sigmoid and power law functionally graded beams", *Steel Compos. Struct.*, **30**(6), 603-615. https://doi.org/10.12989/scs.2019.30.6.603.

Baferani, H.A., Saidi, A.R. and Ehteshami, H. (2011), "Accurate solution for free vibration analysis of functionally graded thick rectangular plates resting on elastic foundation", *Compos. Struct.,* **93**(7), 1842-1853. http://doi.org/10.1016/j.compstruct.2011.01.020.

Carrera, E., Brischetto, S. andRobaldo, A. (2008), "Variable Kinematic Model for the Analysis of Functionally Graded Material plates", *AIAA J.*, **46**(1), 194-203. http://doi.org/10.2514/1.32490.

Carrera, E., Brischetto, S., Cinefra, M. and Soave, M. (2011), "Effects of thickness stretching in functionally graded plates and shells", *Compos. Part B: Eng.*, **42**(2), 123-133. http://doi.org/10..1016/j.compositesb.2010.10.005.

Chen, C.S., Hsu, C.Y. and Tzou, GJ. (2009), "Vibration and stability of functionally graded plates based on a higher-order deformation theory", *J. Reinf. Plast. Compos.*, **28**(10), 1215-1234. https://doi.org/10.1177/0731684408088884.

Dehshahri, K., Nejad, M. Z., Ziaee, S., Niknejad, A. and Hadi, A. (2020), "Free vibrations analysis of arbitrary three-dimensionally FGM nanoplates", *Adv. Nano Res.*, **8**(2), 115-134. https://doi.org/10.12989/anr.2020.8.2.115.

Ebrahimi, T., Nejad, M.Z., Jahankohan, H. and Hadi, A. (2021), "Thermoelastoplastic response of FGM linearly hardening rotating thick cylindrical pressure vessels", *Steel Compos. Struct.*, **38**(2), 189-211. https://doi.org/10.12989/scs.2021.38.2.189.

Fallah, A., Aghdam, M.M. and Kargarnovin, M.H. (2013), "Free vibration analysis of moderately thick functionally graded plates on elastic foundation using the extended Kantorovich method", *Arch. Appl. Mech.*, **83**(2), 177-191. https://doi.org/10.1007/s00419-012-0645-1.

Fares, M.E., Elmarghany, M.K. and Atta, D. (2009), "An efficient and simple refined theory for bending and vibration of functionally graded plates", *Compos. Struct.*, **91**(3), 296-305. https://doi.org/10.1016/j.compstruct.2009.05.008.

Fenjan, R.M., Faleh, N.M. and Ahmed, R.A. (2020b), "Geometrical imperfection and thermal effects on nonlinear stability of microbeams made of graphene-reinforced nano-composites", *Adv. Nano Res.*, **9**(3). 147-156. http://doi.org/10.12989/anr.2020.9.3.147.

Fenjan, R.M., Faleh, N.M. and Ahmed R.A. (2020c), "Strain gradient based static stability analysis of composite crystalline shell structures having porosities", *Steel Compos. Struct.*, **36**(6), 631-642. http://doi.org/10.12989/scs.2020.36.6.631.

Fenjan, R.M., Moustafa, N.M. and Faleh, N.M. (2020a), "Scale-dependent thermal vibration analysis of FG beams having porosities based on DQM", *Adv. Nano Res.*, **8**(4), 283-292. http://doi.org/10.12989/anr.2020.8.4.283.

Ferreira, A.J.M., Carrera, E., Cinefra, M., Roque, C.M.C. and Polit, O. (2011), "Analysis of laminated shells by a sinusoidal shear deformation theory and radial basis functions collocation, accounting for through-the-thickness deformations", *Compos. Part B: Eng.*, **42**(5), 1276-1284. https://doi.org/10.1016/j.compositesb.2011.01.031.

Ferreira, A.J.M., Roque, C.M.C. and Jorge, R.M.N. (2005), "Analysis of composite plates by trigonometric shear deformation theory and multiquadrics", *Comput. Struct.*, **83**(27), 2225–2237. https://doi.org/10.1016/j.compstruc.2005.04.002.

Hirwani, C.K., Panda, S.K. and Mahapatra, T.R. (2018a). "Nonlinear finite element analysis of transient behaviour of delaminated composite plate", *J. Vib. Acoust.*, **140**(2). https://doi.org/10.1115/1.4037848.

Hirwani, C.K., Panda, S.K., Mahapatra, T.R. and Mahapatra, S.S. (2017), "Nonlinear transient finite-element analysis of delaminated composite shallow shell panels", *AIAA J.*, **55**(5), 1734-1748. https://doi.org/10.2514/1.J055624.

Hirwani, C.K., Panda, S.K. and Mahapatra, T.R. (2018b). "Thermomechanical deflection and stress responses of delaminated shallow shell structure using higher-order theories", *Compos. Struct*., **184**, 135-145. S0263822317325023 https://doi.org/10.1016/j.compstruct.2017.09.071.

Hirwani, C.K. and Panda, S.K. (2018), "Numerical and experimental validation of nonlinear deflection and stress responses of pre-damaged glass-fibre reinforced composite structure", *Ocean Eng.*, **159**, 237-252. https://doi.org/10.1016/j.oceaneng.2018.04.035.

Hirwani, C.K. and Panda, S.K. (2019a), "Nonlinear finite element solutions of thermoelastic deflection and stress responses of internally damaged curved panel structure", *Appl. Math. Model.*, **65**, 303-317. S0307904X18304037. https://doi.org/10.1016/j.apm.2018.08.014.

Hirwani, C.K. and Panda, S.K. (2019b), "Nonlinear transient analysis of delaminated curved composite structure under blast/pulse load", *Eng. with Comput.*, 1-14. https://doi.org/10.1007/s00366-019-00757-6.

Hirwani, C.K., Panda, S.K., Mahapatra, S.S., Mandal, S.K., Srivastava, L. and Buragohain, M.K. (2018c), "Flexural strength of delaminated composite plate - An experimental validation", *Int. J. Damage Mech.*, **27**(2), 296-329. 1056789516676515. https://doi.org/10.1177/1056789516676515.

Hirwani, C.K., Panda, S.K., Mahapatra, T.R., Mandal, S.K., Mahapatra, S.S. and De, A.K. (2018e), "Delamination effect on flexural responses of layered curved shallow shell panel-experimental and numerical analysis", *Int. J. Comput. Method.*, **15**(4), 1850027. https://doi.org/10.1142/S0219876218500275.

Hirwani, C.K., Panda, S.K., Mahapatra, T.R. and Mahapatra, S.S. (2017b). "Numerical study and experimental validation of dynamic characteristics of delaminated composite flat and curved shallow shell structure", *J. Aerosp. Eng.*, **30**(5), 04017045. https://doi.org/10.1061/(ASCE)AS.1943-5525.0000756.

Hirwani, C.K., Panda, S.K. and Patle, B.K. (2018d), "Theoretical and experimental validation of nonlinear deflection and stress responses of an internally debonded layer structure using different higher-order theories", *Acta Mechanica*, **229**(8), 3453-3473. https://doi.org/10.1007/s00707-018-2173-8.

Hosseini-Hashemi, S., Rokni Damavandi Taher, H., Akhavan, H. and Omidi, M. (2010), "Free vibration of functionally graded rectangular plates using first-order shear deformation plate theory", *Appl. Math. Model.*, **34**(5), 1276-1291. https://doi.org/10.1016/j.apm.2009.08.008.

Jha, D.K., Kant, T. and Singh, R.K. (2013), "Free vibration response of functionally graded thick plates with shear and normal deformations effects", *Compos. Struct.*, **96**, 799-823. https://doi.org/10.1016/j.compstruct.2012.09.034.

Kar, V.R. and Panda, S.K. (2015), "Nonlinear flexural vibration of shear deformable functionally graded spherical shell panel", *Steel Compos. Struct.,* **18**(3), 693-709. https://doi.org/10.12989/scs.2015.18.3.693.

Karakoti, A., Pandey, S. and Kar, V.R. (2021), "Dynamic responses analysis of P and S-FGM sandwich cylindrical shell panels using a new layerwise method", *Struct. Eng. Mech*., **80**(4), 417-432. https://doi.org/10.12989/sem.2021.80.4.417.

Karami, B. and Janghorban, M. (2019), "A new size-dependent shear deformation theory for wave propagation analysis of triclinic nanobeams", *Steel Compos. Struct*., **32**(2), 213-223.

https://doi.org/10.12989/scs.2019.32.2.213.

Karami, B. and Karami, S. (2019), "Buckling analysis of nanoplate-type temperature-dependent heterogeneous materials", *Adv. Nano Res.*, **7**(1), 51-61. https://doi.org/10.12989/anr.2019.7.1.051.

Katariya, P.V., Hirwani, C.K. and Panda, S.K. (2019), "Geometrically nonlinear deflection and stress analysis of skew sandwich shell panel using higher-order theory", *Eng. with Compu.*, **35** (2), 467-485. https://doi.org/10.1007/s00366-018-0609-3.

Katariya, P.V., Mehar, K. and Panda, S.K. (2020), "Nonlinear dynamic responses of layered skew sandwich composite structure and experimental validation", *Int. J. Nonlinear Mech.*, **125**, 103527. https://doi.org/10.1016/j.ijnonlinmec.2020.103527.

Katariya, P.V. and Panda, S.K. (2019a), "Numerical evaluation of transient deflection and frequency responses of sandwich shell structure using higher order theory and different mechanical loadings", *Eng. with Comput.*, **35**(3), 1009-1026. https://doi.org/10.1007/s00366-018-0646-y.

Katariya, P.V. and Panda, S.K. (2019b), "Numerical frequency analysis of skew sandwich layered composite shell structures under thermal environment including shear deformation effects", *Struct. Eng. Mech*., **71**(6), 657-668. https://doi.org/10.12989/sem.2019.71.6.657.

Koizumi, M. (1997), "FGM activities in Japan", *Compos. Part B: Eng*, **28**, 1–4. https://doi.org/10.1016/S1359-8368(96)00016-9.

Kolahchi, R., Safari, M. and Esmailpour, M. (2016), "Dynamic stability analysis of temperature-dependent functionally graded CNT-reinforced visco-plates resting on orthotropic elastomeric medium", *Compos. Struct.*, **150**, 255-265. https://doi.org/10.1016/j.compstruct.2016.05.023.

Liu, W., Liu, S., Fan, M., Tian, W., Wang, J. and Tahouneh, V. (2020), "Influence of internal pores and graphene platelets on vibration of non-uniform functionally graded columns", *Steel Compos. Struct.*, **35**(2), 295-303. https://doi.org/10.12989/scs.2020.35.2.295.

Madenci, E. (2019), "A refined functional and mixed formulation to static analyses of fgm beams", *Struct. Eng. Mech.*, **69**(4), 427-437. https://doi.org/10.12989/sem.2019.69.4.427

Mansour, W and Fayed, S. (2021), "Flexural rigidity and ductility of RC beams reinforced with steel and recycled plastic fibers", *Steel Compos. Struct.*, **41**(3), 317-334. https://doi.org/10.12989/scs.2021.41.3.317.

Mantari, J.L. and Guedes Soares, C. (2012), "Generalized hybrid quasi-3D shear deformation theory for the static analysis of advanced composite plates", *Compos. Struct.*, **94**(8), 2561-2575. https://doi.org/10.1016/j.compstruct.2012.02.019.

Mantari, J.L. and Guedes Soares, C. (2013), "A novel higher-order shear deformation theory with stretching effect for functionally graded plates", *Compos. Part B: Eng.*, **45**(1), 268-281. https://doi.org/10.1016/j.compositesb.2012.05.036.

Mantari, J.L., Oktem, A.S. and Guedes Soares, C. (2012), "Bending response of functionally graded plates by using a new higher order shear deformation theory", *Compos. Struct.*, **94**(2), 714-723. https://doi.org/10.1016/j.compstruct.2011.09.007.

Mercan, K., Ebrahimi, F. and Civalek, Ö. (2020), "Vibration of angle-ply laminated composite circular and annular plates", *Steel Compos. Struct.*, **34**(1), 141-154. https://doi.org/10.12989/scs.2020.34.1.141.

Mindlin, R.D. (1951), "Influence of rotatory inertia and shear on flexural motions of isotropic, elastic plates", *J. Appl. Mech.*, **18**(1), 31-38.

Natarajan, S. and Manickam, G. (2012), "Bending and vibration of functionally graded material sandwich plates using an accurate theory", *Finite Elem. Anal. Des.*, **57**, 32–42. https://doi.org/10.1016/j.finel.2012.03.006.

Neves, A.M.A., Ferreira, A.J.M., Carrera, E., Cinefra, M., Roque, C.M.C., Jorge, R.M.N. and Soares, C.M.M. (2013), "Static, free vibration and buckling analysis of isotropic and sandwich functionally graded plates using a quasi-3D higher-order shear deformation theory and a meshless technique", *Compos. Part B: Eng*., **44**(1), 657-674. ttps://doi.org/10.1016/j.compositesb.2012.01.089.

Neves, A.M.A., Ferreira, A.J.M., Carrera, E., Cinefra, M., Roque, C.M.C., Jorge, R.M.N. and Soares, C.M.M. (2012b), "A quasi-3D hyperbolic shear deformation theory for the static and free vibration analysis of functionally graded plates", *Compos. Struct*., **94**(5), 1814-1825. https://doi.org/10.1016/j.compstruct.2011.12.005.

Neves, A.M.A., Ferreira, A.J.M., Carrera, E., Roque, C.M.C., Cinefra, M., Jorge, R.M.N. and Soares, C.M.M. (2012a), "A quasi-3D sinusoidal shear deformation theory for the static and free vibration analysis of functionally graded plates", *Compos. Part B: Eng*., **43**(2), 711-725. ttps://doi.org/10.1016/j.compositesb.2011.08.009.

Noroozi, R., Barati, A., Kazemi, A., Norouzi, S. and Hadi, A. (2020), "Torsional vibration analysis of bi-directional FG nano-cone with arbitrary cross-section based on nonlocal strain gradient elasticity", *Adv. Nano Res*., **8**(1), 13-24. https://doi.org/10.12989/anr.2020.8.1.013.

Othman, M. and Fekry, M. (2018), "Effect of rotation and gravity on generalized thermo-viscoelastic medium with voids", *Multidiscip. Model. Mater. Struct.*, **14**(2), 322-338. ttps://doi.org/10.1108/MMMS-08-2017-0082.

Pandey, H.K., Agrawal, H., Panda, S.K., Hirwani, C.K., Katariya, P.V. and Dewangan, H.C. (2020), "Experimental and numerical bending deflection of cenosphere filled hybrid (Glass/Cenosphere/Epoxy) composite", *Struct. Eng. Mech.*, **73** (6), 715-724. https://doi.org/10.12989/sem.2020.73.6.715.

Panjehpour, M., Loh, E.W.K. and Deepak, T.J. (2018), "Structural insulated panels: state-of-the-art", *Trends Civil Eng. its Architect.*, **3**(1) 336-340. ttps://doi.org/10.32474/TCEIA.2018.03.000151.

Pasternak, P.L. (1954), "On a new method of analysis of an elastic foundation by means of two foundation constants", Gosuedarstvennoe Izadatelstvo Literatim po Stroitelstvu i Arkhitekture, **1**, 1-56.

Patle, B.K., Hirwani, C.K., Panda, S.K., Katariya, P.V., Dewangan, H.C. and Sharma, N. (2020), "Nonlinear deflection responses of layered composite structure using uncertain fuzzified elastic properties", *Steel Compos. Struct*., **35**(6), 753-763. https://doi.org/10.12989/scs.2020.35.6.753.

Patnaik, S.S., Swain, A. and Roy, T. (2020), "Creep compliance and micromechanics of multi-walled carbon nanotubes based hybrid composites", *Compos. Mater. Eng*., **2**(2), 141-152. ttps://doi.org/10.12989/cme.2020.2.2.141.

Qian, L.F. and Batra, R.C. (2005), "Three-dimensional transient heat conduction in a functionally graded thick plate with a higher-order plate theory and a meshless local Petrov-Galerkin Method", *Comput. Mech.*, **35**(3), 214-226. https://doi.org/10.1007/s00466-004-0617-6.

Rachedi, M.A., Benyoucef, S., Bouhadra, A., Bachir Bouiadjra, R., Sekkal, M. and Benachour, A. (2020), "Impact of the homogenization models on the thermoelastic response of FG plates on variable elastic foundation", *Geomech. Eng.*, **22**(1), 65-80. https://doi.org/10.12989/gae.2020.22.1.065.

Rashidpour, P., Ghadiri, M. and Zajkani, A. (2021), "The response of viscoelastic composite laminated microplate under low-velocity impact based on nonlocal strain gradient theory for different boundary conditions", *Steel Compos. Struct.*, **41**(3), 335-351. https://doi.org/10.12989/scs.2021.41.3.335.

Reddy, J.N. (2000), "Analysis of functionally graded plates", *Int. J. Numer. Method. Eng.*, **47**(1-3), 663-684. https://doi.org/10.1002/(SICI)1097-

0207(20000110/30)47:1/3<663::AID-NME787>3.0.CO;2-8.
Reddy, J.N. (2011), "A general nonlinear third-order theory of functionally graded plates", *Int. J. Aerosp. Lightweight Struct.*, **1**(1), 1-21. https://doi.org/10.3850/S201042861100002X.
Reissner, E. (1945), "The effect of transverse shear deformation on the bending of elastic plates", *J. Appl. Mech.*, **12**(2), 69-72.
Sadoughifar, A., Farhatnia, F., Izadinia, M. and Talaeetaba, S.B. (2020), "Size-dependent buckling behaviour of FG annular/circular thick nanoplates with porosities resting on Kerr foundation based on new hyperbolic shear deformation theory", *Struct. Eng. Mech.*, **73**(3), 225-238. https://doi.org/10.12989/sem.2020.73.3.225.
Sahoo, S.S., Panda, S.K., Mahapatra, T.R. and Hirwani, C.K. (2019), "Numerical analysis of transient responses of delaminated layered structure using different mid-plane theories and experimental validation", *Iran J. Sci. Technol. T. Mech. Eng.*, **43**,41-56. https://doi.org/10.1007/s40997-017-0111-3.
Selmi, A. (2020), "Dynamic behavior of axially functionally graded simply supported beams", *Smart Struct. Syst.*, **25**(6), 669-678. https://doi.org/10.12989/sss.2020.25.6.669.
Shahmohammadi, M.A., Azhari, M. and Saadatpour, M.M. (2020), "Free vibration analysis of sandwich FGM shells using isogeometric B-spline finite strip method", *Steel Compos. Struct.*, **34**(3), 361-376. https://doi.org/10.12989/scs.2020.34.3.361.
Shakouri, M. (2021), "Analytical solution for stability analysis of joined cross-ply thin laminated conical shells under axial compression", *Compos. Mater. Eng.*, **3**(2), 117-134. https://doi.org/10.12989/cme.2021.3.2.117.
Singh, V.K., Hirwani, C.K., Panda, S.K., Mahapatra, T.R. and Mehar, K. (2019), "Numerical and experimental nonlinear dynamic response reduction of smart composite curved structure using collocation and non-collocation configuration", *Proceedings of the Institution of Mechanical Engineers, Part C: Journal of Mechanical Engineering Science*, **233**(5), 095440621877436–. doi:10.1177/0954406218774362.
Sobhy, M. (2013), "Buckling and free vibration of exponentially graded sandwich plates resting on elastic foundations under various boundary conditions", *Compos. Struct.*, **99**, 76-87. https://doi.org/10.1016/j.compstruct.2012.11.018.
Talha, M. and Singh, B.N. (2010), "Static response and free vibration analysis of FGM plates using higher order shear deformation theory", *Appl. Math. Model.*, **34**(12), 3991-4011. https://doi.org/10.1016/j.apm.2010.03.034.
Thai, H.T. and Choi, D.H. (2012), "A refined shear deformation theory for free vibration of functionally graded plates on elastic foundation", *Compos. Part B: Eng.,* **43**(5), 2335-2347. https://doi.org/10.1016/j.compositesb.2011.11.062.
Thai, H.T. and Choi, D.H. (2014), "Zeroth-order shear deformation theory for functionally graded plates resting on elastic foundation", *Int. J. Mech. Sci.*, **78**, 35-43. ttps://doi.org/10.1016/j.ijmecsci.2013.09.020.
Thai, H.T. and Choi, D.H. (2011), "A refined plate theory for functionally graded plates resting on elastic foundation", *Compos. Sci. Technol.*, **71**(16), 1850-1858. https://doi.org/10.1016/j.compscitech.2011.08.016.
Thai, H.T. and Kim, S.E. (2013), "A simple quasi-3D sinusoidal shear deformation theory for functionally graded plates", *Compos. Struct.*, **99**, 172-180. https://doi.org/10.1016/j.compstruct.2012.11.030.
Timesli, A. (2020), "An efficient approach for prediction of the nonlocal critical buckling load of double-walled carbon nanotubes using the nonlocal Donnell shell theory", *SN Appl. Sci.*, **2**, 407. https://doi.org/10.1007/s42452-020-2182-9
Wang, H., Yan, W. and Li, C. (2020), "Response of angle-ply laminated cylindrical shells with surface-bonded piezoelectric layers", *Struct. Eng. Mech.*, **76**(5), 599-611. https://doi.org/10.12989/SEM.2020.76.5.599.
Winkler, E. (1867), "Die lehre von der elasticitaet und festigkeit", Prague: Prag Dominicus; 1867.
Xiang, S., Jin, Y.X., Bi, Z.Y., Jiang, S.X. and Yang, M.S. (2011), "A n-order shear deformation theory for free vibration of functionally graded and composite sandwich plates", *Compos. Struct.*, **93**(11), 2826-2832. https://doi.org/10.1016/j.compstruct.2011.05.022.
Xiang, S. and Kang, G.W. (2013), "A nth-order shear deformation theory for the bending analysis on the functionally graded plates", *Eur. J. Mech.–A/Solids*, **37**, 336-343. https://doi.org/10.1016/j.euromechsol.2012.08.005.
Yuan, Y., Zhao, K., Zhao, Y. and Kiani, K. (2020), "Nonlocal-integro-vibro analysis of vertically aligned monolayered nonuniform FGM nanorods", *Steel Compos. Struct.*, **37**(5), 551-569. https://doi.org/10.12989/SCS.2020.37.5.551.
Zenkour, A.M. (2009), "The refined sinusoidal theory for FGM plates on elastic foundations", *Int. J. Mech. Sci.*, **51**(11-12), 869-880. https://doi.org/10.1016/j.ijmecsci.2009.09.026.

CC